European Biophysics Journal (2020) 49:571–589
https://doi.org/10.1007/s00249-020-01463-8

ORIGINAL ARTICLE

Energetic and thermodynamical aspects of the cyclodextrins-cannabidiol complex in aqueous solution: a molecular-dynamics study

A. J. da Silva[1] · E. S. dos Santos[2]

Received: 8 June 2020 / Revised: 23 August 2020 / Accepted: 4 September 2020 / Published online: 16 September 2020

Abstract
Cyclodextrins (CDs) are well-known carriers for encapsulating hydrophobic molecules, while among cannabinoids, cannabidiol (CBD) has attracted considerable attention due to its therapeutic capability. In this framework, we employed molecular dynamics and docking techniques for investigating the interaction energy and thermodynamical issues between different CDs (α, β, and γ type) and CBD immersed in water and a solution mimicking a physiological environment. We quantified the energetic aspects, for different thermal conditions, in which both aqueous solutions interact with CBDs and CDs and the CBD-CDs complex itself. In order to approximate the physiological conditions, our simulations also included the mammalian temperature. The calculations revealed significant interaction energy between lactate and the CD surface and a movement of lactate toward CD as well. We observed an almost constant number of lactate molecules forming clusters without exhibiting a temperature dependence. Next, the degree of CBD-CDs complexation at four different temperatures was analyzed. The results showed that the complexation depends on the medium, becoming weaker with the temperature increment. Our findings highlighted that the entropy contribution is relevant for CBD-α-CD and CBD-β-CD, while CBD-γ-CD is practically insensitive to temperature changes for both solutions. In both water and artificial physiological solutions, the γ-CD appears more stable than the other complexes. Overall, CBD achieved partial encapsulation considering α-CD and β-CD, showing a temperature dependence, while γ-CD remained fully immersed no matter the thermal level assumed. We also discuss the pharmacological relevance and physiological implications of these findings.

Keywords Ringer's lactate solution · Cyclodextrin · Cannabidiol · Molecular dynamics · Docking · Temperature

Introduction

Research into thermal effects is relevant for understanding several physiological mechanisms, such as allowing an appropriate design of different drugs. In cell biology, temperature regulates the biochemical pathways by modulating membrane fluidity, protein stability, ion channels, and receptors dynamics, among others (Mundt et al. 2018; Rosa et al. 2017; Hubbard et al. 1971; Lee and Deutsch 1990; Murata and Los 1997). Specifically, in brain tissue the metabolic activity remains a complex issue in physiology because the neuronal activity is critically dependent on the on the thermal levels (Kiyatkin 2019; Brooks 1983; Horel 1996). Consequently, experimental paradigms employing thermal regulation still represent an excellent strategy to uncover many interesting biophysical properties in both physiological and pharmacological contexts (Bikkina et al. 2017; Schiff and Somjen 1985; Andersen and Moser 1995; Yang and Wang 2006). From this evidence, it is clear that temperature variation can provide a suitable method of manipulating interactions between molecules and their surrounding environment.

Nowadays, numerous studies still focus on the physicochemical properties of aqueous systems, considering high concentrations of only a few ionic species (Zasetsky and

Electronic supplementary material The online version of this article (https://doi.org/10.1007/s00249-020-01463-8) contains supplementary material, which is available to authorized users.

✉ A. J. da Silva
adjesbr@ufsb.edu.br

[1] Instituto de Humanidades, Artes e Ciências, Universidade Federal do Sul da Bahia, Itabuna, Bahia 45613-204, Brazil

[2] Instituto de Física, Universidade Federal da Bahia, Campus Universitário de Ondina, Salvador, Bahia 40210-340, Brazil

Svishchev 2001; Payne et al. 1995a, b, c). However, within a more realistic perspective in physiology, it is required to investigate such properties considering dilute solutions composed of ionic species found in physiological fluids. In particular, understanding artificial physiological solutions has been fundamental not only in basic research but also for clinical purposes (Baskett 2003; Ziance et al. 2009). Within this scope, one can highlight the Ringer lactate solution (RL solution), also known as Hartmann or sodium lactate solution, commonly employed in administering intravenous medication (Baskett 2003; Iqbal et al. 2018). This fluid has low hypotonic and caloric levels, being preferred for shock resuscitation, after a blood loss due to trauma (Ichai et al. 2014; Bondoli et al. 1978). Although RL represents a slightly hypotonic and low caloric solution, few side effects have been documented in the literature. For this reason, it becomes relevant to quantify how pharmaceuticals and proteins interact with the RL constituents.

Experimental work has been an important procedure in uncovering biophysical aspects of the ionic interactions with natural and synthetic molecules. For example, solubility decrement promotes changes in the melting temperature of proteins (Kramer et al. 2012). Reports also revealed how calcium ions interact with the family of gastrin peptide hormones, considering both immersed in two different organic liquids (Peggion et al. 1983). Last, but not least, a subsequent thermodynamic study also clarified the magnesium interplay with human growth hormone, showing a protein thermal stability increment in the presence of this ion (Saboury et al. 2006).

Although there is a wealth of literature, quantified by different experimental work, valuable information about ion-protein interactions was also achieved using simulation methods (Gunsteren and Mark 1992). In this sense, thanks to the extensive development of analytical and numerical methods, molecular dynamics and molecular docking have been vastly applied in recent years (Durrant and McCammon 2011). Both methodologies allow for the translation of physical laws representing the biological system into a faithful mechanistic representation of experimental results. Another remarkable advantage of the in-silico approach is the opportunity to access refined mechanisms inaccessible by empirical protocols. In this context, computational simulations represent a useful procedure to investigate protein interaction with aqueous solution components in distinct physicochemical conditions (Fraternali and van Gunsteren 1996; Soares et al. 2003). Among applications based on physiological motivation, simulations enabled the examination of how sodium and chloride propagation is processed near the lysosome surface (Friedman 2011). Among the broad spectrum of possibilities, theoretical studies involving CDs solubility in aqueous solutions also emerge as a relevant field due to their industry and research applications. Mainly, simulations are necessary for understanding the encapsulation mechanism of hydrophobic molecules into CDs, providing valuable data to be used by the pharmaceutical industry and basic science.

Molecular docking is credited as a powerful approach for structure-based drug discovery. It constitutes a suitable method to predict and confirm important biophysical properties, useful for a better comprehension of the complex formed between CDs and different molecules (Kitchen et al. 2004; Meng et al. 2011), such as in systems in which the size did not drastically diverge from our work, where the results predicted reinforced the experimental findings. For example, Chung et al. (2019) and Elmes et al. (2015) used docking to study how cannabidiol modulates the effects of delta-9-tetrahydrocannabinol (Δ-9-THC or THC) on the cannabinoid receptor type 1 and fatty acid-binding proteins, respectively. Furthermore, Chaudhuri et al. (2010) combined docking, semi-empirical calculations, and fluorescence spectroscopic, to give detailed insights into the serotonin encapsulation mechanism in the β-CD cavity. Docking has been successfully applied by Upadhye et al. (2010) which who also combined experimental and theoretical investigation, to study the THC inclusion into β-CD. The same study showed that employing molecular docking is still the most probable mode of THC binding with β-CD. Also, it is important to mention that many studies using molecular docking were carried out in encapsulation of different molecules within α-CD (Cai et al. 2001), β-CD (Chen et al. 2019), and γ-CD (Pahari et al. 2018), respectively. Thus, when carefully used, molecular docking represents a robust methodology for investigating the CBD inclusion in CDs.

The compound THC is a lipophilic molecule with active principle extracted from the leaves of the plant *Cannabis sativa*, which is used for both recreational and pharmacological purposes (Hadland et al. 2015; Baron 2015). In humans, moderate consumption of this substance produces periods of euphoria followed by relaxation, while higher doses lead to a predominantly depressive effect (Ameri 1999). Although many different mechanisms have been discovered, it is well known that cannabinoids modify molecular mechanisms related to learning and memory processes in the hippocampus (Riedel and Davies 2005). This evidence of its direct action in the central nervous system trigged an intense study to synthesize substances, mimicking the pharmacological effects, according to those observed in THC. Furthermore, it was required to make the identification and characterization of the binding sites of these substances (Freund et al. 2003). In this framework, two important independent studies carried out in the rat nervous system identified the cannabinoid binding site and cloned the first G protein-coupled receptor known as CB1 or cannabinoid receptor type 1 (Devane et al. 1992; Matsuda et al. 1990). Later, Munro et al. (1993) reported another receptor cloned into cells of the immune

system, known by CB2 receptors. The discovery of CB2 was particularly remarkable because it has enabled a better understanding of the effects of cannabinoids relative to the peripheral system. Naturally, with the identification and localization of cannabinoids receptors, the next step was to find and further characterize the endogenous and exogenous cannabinoids. In this sense, the first endocannabinoid discovered was called anandamide or arachidonyl-ethanolamide (AEA) (Devane et al. 1992). Further studies by Sugiura et al. (1995, 2001) showed that 2-arachidonylglycerol (2-AG) competes with the AEA for the same cannabinoid receptor, thus confirming the presence of another endocannabinoid in mammals.

The biosynthesis of both endocannabinoids is a matter of intense studies, being mainly associated with two processes. The first is related to the elevation of the intracellular calcium ions (Ca^{2+}) concentration (Lenz et al. 1998), which originated from the stocks of the endoplasmic reticulum and the entrance of Ca^{2+} (Llano et al. 1991). About the production of cannabinoids, the exact mechanism for the recruitment of a high concentration of intracellular Ca2 + is not accurately known yet (Xu and Xen 2015). Relative to the other process, the presence of metabotropic type 1 glutamate receptors (mGluR1) or muscarinic acetylcholine receptors (mAChR) activate enzymes in the intracellular environment, such as phospholipase C, hydrolyzes the cellular membrane, giving the precursor molecules required for the endocannabinoid synthesis (Chevaleyre et al. 2006). The produced molecules perform a retrograde diffusion, where they bind to receptors located at the axon terminal and suppress the neurotransmission machinery. The attenuation in neurotransmitter release occurs because CB1 receptors interact with potassium and calcium channels via G protein (Pitler and Alger 1994). Electrophysiological studies in the hippocampus and cerebellum of rats reported, during a repetitive electrical stimulus, suppression of the postsynaptic potentials that the same cell receives. This intriguing phenomenon is defined as depolarization-induced suppression of inhibition (DSI) (Pitler and Alger 1992; Vincent et al. 1992). Surprisingly, subsequent research on glutamatergic synapses revealed a suppressive effect of excitatory levels later defined as depolarization-induced suppression of excitation (DSE) (Kreitzer and Regehr 2001; Maejima et al. 2001; Levenes et al. 2001). Thus, the richness and complexity of cannabinoid mechanisms is evident, opening up plenty of room for theoretical studies investigating how these substances interact with the components of physiological fluids and artificial aqueous solutions.

The large variety of synthetic cannabinoids and their therapeutic potential encouraged a deeper investigation of these substances. Among phytocannabinoids, one can highlight CBD thanks to its potential benefits in post-traumatic stress disorder, anxiety, pain, and epilepsy (Elms et al. 2019; Lee et al. 2017; Hammell et al. 2016; Silvestro et al. 2019; Burstein 2015). Unlike other psychoactive compounds, a CBD remarkable advantage includes the absence of euphoric effects commonly linked to THC use. Recently, in vitro studies, involving extracellular field potential recordings, suggest that CBD induce long-term potentiation in the CA1 region of the mice hippocampal slices (Maggio et al. 2018).

Furthermore, in the amygdala, there was an enhancement of spine densities modified after the administration of CBD (Uhernik et al. 2018). However, despite the unquestionable importance of CBD in pharmacology, CBD's poor solubility in aqueous solutions still represents obstacles for clinical applications and in vitro investigations. In fact, electrophysiological experiments, performed in brain slices, frequently require a tissue immersion in hydrophilic solutions such as artificial cerebrospinal fluid. Thus, CBD application in hydrophobic environment requires an appropriate host compound as an efficient way to enhance their water bioavailability and solubility.

The CDs molecules are endowed with a hydrophilic outer surface and a hydrophobic inner cavity, forming a toroidal shape. There are three natural CD types: α, β and γ, consisting of six, seven and eight α-(1,4)-linked glycosyl units, respectively. The peculiar architecture of CD is propitious to form encapsulation complexes with a vast range of guest molecules. CDs are a product of enzymatic degradation of starch by glucanotransferase (Valle 2004), being practically nontoxic, appropriate in food industry, cosmetics, personal care, and toiletry (Gidwani and Vyas 2015). After complexes of CDs are formed, drugs have their physicochemical properties modified as, for instance, solubility and stability. In pharmaceutics, CDs complexation is employed in the enhancement of aqueous solubility of lipophilic drugs. Due to this undoubted importance, in different fields of knowledge, numerous efforts have been devoted to characterizing CD using experimental and theoretical approaches. For instance, Hingerty et al. (1984) performed a detailed study on α, β and γ-CD using neutron diffraction, revealing that hydrogen bonds exhibit dynamical behavior even in the solid state. Experimental investigation has also contemplated the thermal effects on CD, as reported by Steffens et al. (2007) who studied, how *N*-adamantylacrylamide was complexed with β-CD at different temperatures. Moreover, Ishiwata and Kamyia, using fluorimetric data and a temperature range of 288.15–313.15 K, investigated the influence between warfarin and the coumachlor complex in β-CD (Ishiwata and Kamyia 1998). Furthermore, simulations also contributed to reveal several biophysical details of the thermal effects on CDs (Koehler et al. 1987). Finally, using molecular dynamics simulations, Winkler et al. (2000) studied how the hydration process depends on temperature variation β-CD. Overall, motivated by the explanations given above, the present work intends to carry out theoretical investigations

to characterize how different temperatures may modulate CBD-CDs complexation immersed in water and RL solution.

Materials and methods

Docking simulation

Docking simulations of CBD (COD-CID 13956-29-1) into targets α-CD (COD-CID 444913), β-CD (COD-CID 444041), and γ-CD (COD-CID 5287407) were based on three-dimensional structures from PubChem (https://pubchem.ncbi.nlm.nih.gov/) in the "SDF" file format. OpenBabel version 2.3.1 converted CD and CBD representations into the PDB format (O'Boyle et al. 2011). For these original structures, polar hydrogen atoms were added using the AutodockTools (Morris et al. 2009), and partial charges were calculated using empirical force field MMFF94 (Halgren 1999). We considered six degrees of freedom for CBD with all CDs being rigid.

Docking simulations employed the Autodock Vina version 1.1.2 (Trott and Olson 2010), where the simulation boxes were defined around the coordinates of the CDs centers with size 40 Å in each direction and a grid spacing of 0.375 Å. The box was created in such a way that it was sufficiently large to include not only the respective cavities of the CDs but also the structure of the CBD. Table 1 shows the best parameters applied to adjust CBD docking into CD with the energy range specifying the maximum number of binding modes to the output. Identical solutions in terms of conformation were divided into families, where the best modes of binding were chosen by adopting the lowest binding free energy value and visualized through Pymol version 1.4.1. (DeLano 2011). Each complex obtained, taking into account the lowest energy, was subject to new optimization using the Steepest Descent algorithm to increase the accuracy of the results.

Molecular dynamics

The simulations were built using the Gromacs 5.1.2 package, adopting the OPLS-AA force field to the structures taken of the complexes obtained from the docking procedure (Abraham et al. 2016; Jorgensen et al. 1996; Dodda et al. 2017). The CDs, CBD, and lactate topologies were generated by the web LigParGen Server (Jorgensen et al. 1996). The present work considers CBD-α-CD, CBD-β-CD, and CBD-γ-CD complexes immersed into a saline solution, which resembles a RL type, containing the following concentrations: Na^+ (1.66 mmol L^{-1}), Cl^- (1.98 mmol L^{-1}), lactate (7.7 mmol L^{-1}), K^+ (5.4 mmol L^{-1}), and Ca^{2+} (1.44 mmol L^{-1}), such as the same CDs types immersed in only water. The complexes soaked in a volume of 216 nm^3 of cubic boxes, containing 2100 water molecules of the tip3p type in a minimum distance of 1 nm between the complexes and walls. Neutralization of systems was achieved by adding 150 mM of NaCl molecules. The systems were minimized with steepest descent algorithm and equilibrated with restraint position to guarantee the accommodation of the solvent around the complex. We assumed NPT conditions ($T = 298$ K and $P = 1$ bar) during 50 ns, applying periodic boundary conditions (Wardi 1988).

Temperature was maintained constant using Berendsen's method with the time constant of 0.1 ps, while pressure was equilibrated at 1 bar by Berendsen barostat employing 1 ps time constant relaxation (Berendsen et al. 1984). LINCS algorithm was applied for all bonds within the complex allowing 2 fs time steps and SETTLE algorithm was adopted for water molecule bonds (Hess et al. 1997; Miyamoto and Kollman 1992). The cut-off used for the non-bonded interactions was ~ 1 nm with electrostatic interactions computed using the particle mesh Ewald method (Darden et al. 1993). Table S1 shows a compilation of the parameters used in the simulations. The initial velocity was generated from the Maxwell–Boltzmann distribution, while graphs and figures were created employing Origin (OriginLab, Northampton, MA) and V.M.D. version 1.9.1. (Humphrey et al. 1996). We explored the same protocol for all simulations running during 250 ns for four temperatures initiating at 298 K in steps of 12 K until it reached 334 K.

The binding free energies between CBD-CD were calculated using the molecular mechanics (MM) based on Poisson-Boltzmann surface area (MM-PBSA) (Kumari and Kumar 2014). The MM-PBSA approach combines three energetic terms to account for the change in the free energy of binding. ΔG_{bind} was estimated from the free energies of the reactants and product of the reaction according to the equation:

$$\Delta G_{\text{bind}} = \langle G_{\text{PL}} \rangle - \langle G_P \rangle - \langle G_L \rangle, \quad (1)$$

where G_{PL}, G_P and G_L are the total free energy of the protein−ligand complex, total free energies of the isolated protein, and ligand in solvent, respectively. The advantage of MM-PBSA compared to rigorous methods of free energy calculations, like free energy perturbation (FEP) and

Table 1 Parameters used in docking simulations

Parameters	Value
Energy range	10
Num modes	20
Exhaustiveness	8
Seed	− 150

thermodynamic integration (TI), is that these methods are computationally expensive. In this approach, Eq. 1 is estimated from:

$$\Delta G_{\text{bind}} = E_{\text{bond}} + E_{\text{ele}} + E_{\text{vdw}} + G_{\text{pol}} + G_{\text{np}} - T\Delta S, \quad (2)$$

where the first three terms are from the MM energy terms from bonded (bond, angle and dihedral), electrostatic, and van der Waals interactions. G_{pol} and G_{np} are the polar and non-polar contributions to the solvation free energies and the last term refers to entropy. Calculations of binding free energy assumed two approaches: first, considering the CBD-CD complex in an aqueous solution medium, followed by a second, contemplating the CBD-CD complex in the RL solution. Configurational entropy was estimated from trajectory based on the variance–covariance matrix of the atomic positional fluctuations, using a quasi-harmonic method, where the variance–covariance matrix was calculated for all atoms in the complex. In the quasi-harmonic method using Cartesian coordinates, the mass-weighted variance–covariance matrix is first calculated from MD trajectories, in which the overall translations and rotations of the solute molecule are removed using least-squares fits of mass-weighted coordinates (Hikiri et al. 2016).

Let us justify the temperature range used in the present work. From a physiological point of view, thermal changes in vertebrates may be associated with conditions of hypothermia and hyperthermia. As reported by several authors, the study of the interaction of substances at a temperature much higher than that found in physiological patterns is important in the pharmacological domain. For example, Chiang et al. used MD calculations, to assess the temperature dependence of the celecoxib (CCB) and hydroxypropyl-β-CD (HP-β-CD) complexation in water solution (Chiang et al. 2014). Besides assuming room temperature (298 K) these authors also considered 333 K, enabling to document a transition state of CCB and HP-β-CD, showing an exit at a higher temperature of celecoxib and HP-β-CD. Moreover, Steffens et al. (2007) using the interval 323.15–363.15 K, observed that *N*-adamantylacrylamide, when complexed with randomly methylated-β-CD exhibits, below a critical temperature (338.15 K), a polymerized solution predominance. A precipitation mechanism above this temperature leads to an increase in the relative polymerization rate.

Lamparczyk and Zarzycki (1995) adopted a wide range of temperatures (from 5 to 353.15 K) to quantify the temperature impact on the separation of estradiol and equilin by liquid chromatography employing mobile phases modified by β-CD. Finally, Manilla et al. (2007) employed several temperatures within the interval of 323.15–553.15 K, using the precipitation complexation methodology, to obtain a CBD complex with β-CD for sublingual administration. In summary, the temperatures used in the present work are within the thermal levels, in accordance with previous studies involving the formation of the CBD-CD complex. Simulations occurred during 250 ns, using four temperatures initiating at 298 K with a step of 12 K until it achieving 334 K. Finally, the initial velocity was generated from the Maxwell–Boltzmann distribution. Graphs and figures were created employing Origin (OriginLab, Northampton, MA) and V.M.D. version 1.9.1. (Humphrey et al. 1996).

Results and discussion

Docking

The preparation and characterization of a 1:1 stoichiometry of CBD and THC encapsulated in β-CD were independently studied by Mannila et al. (2005), (2007) and Upadhye et al. (2010). Assuming the same stoichiometry, we show that the most likely ways of bonding are the introduction of the methyl group attached to the aromatic ring of CBD within the hydrophobic cavity of α, β-CD (Fig. 1a, b). Moreover, we found that hydrogen bonds play an essential role in the stabilization of complexes, where the interactions between the methyl and hydroxyl group of α, β-CD produce hydrogen bonds (HB) with the energy of − 0.519 and − 0.147 kcal mol^{-1}, respectively. Additionally, CBD is fully inserted in the γ-CD cavity (Fig. 1c) to form HB with total energy − 1028 kcal mol^{-1} (see Table S2 in Supplementary Material) and van der Waals interactions controlling the binding of the CBD with the three CDs.

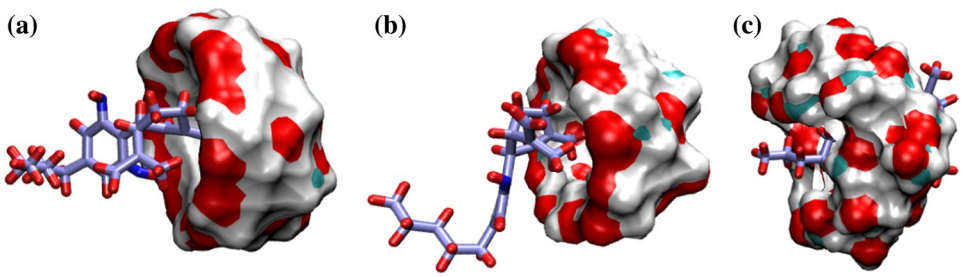

Fig. 1 Binding pose of CBD within the CDs: **a** α-CD-CBD, **b** β-CD-CBD and **c** γ-CD-CBD cavity during the complex formation

System stability

For all systems and temperatures, the energetic stability was confirmed in both water and RL solutions (data not shown). To illustrate this calculation we highlighted kinetic, potential energies as function of time (Figs. 2, 3), and root-mean

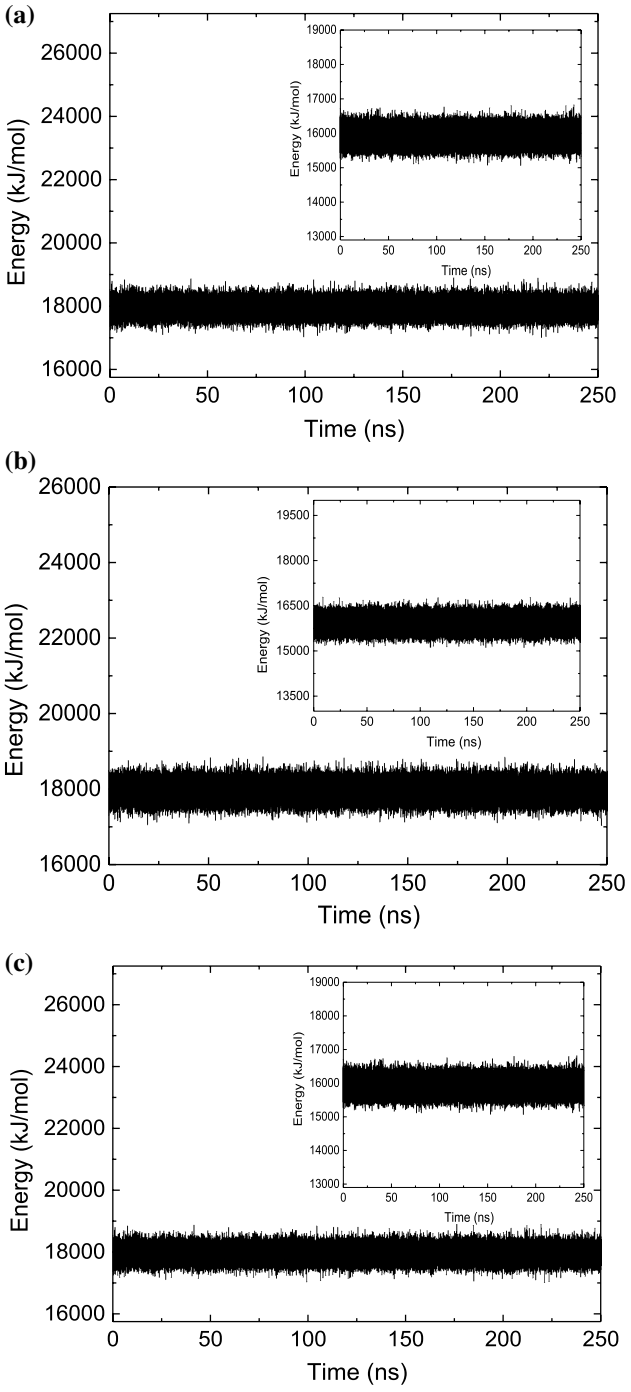

Fig. 2 From up to down three calculations at 310 K, considering the kinetic energies for CDs immersed in RL solution (main panel) and water (inset): **a** α-CD, **b** β-CD, and **c** γ-CD

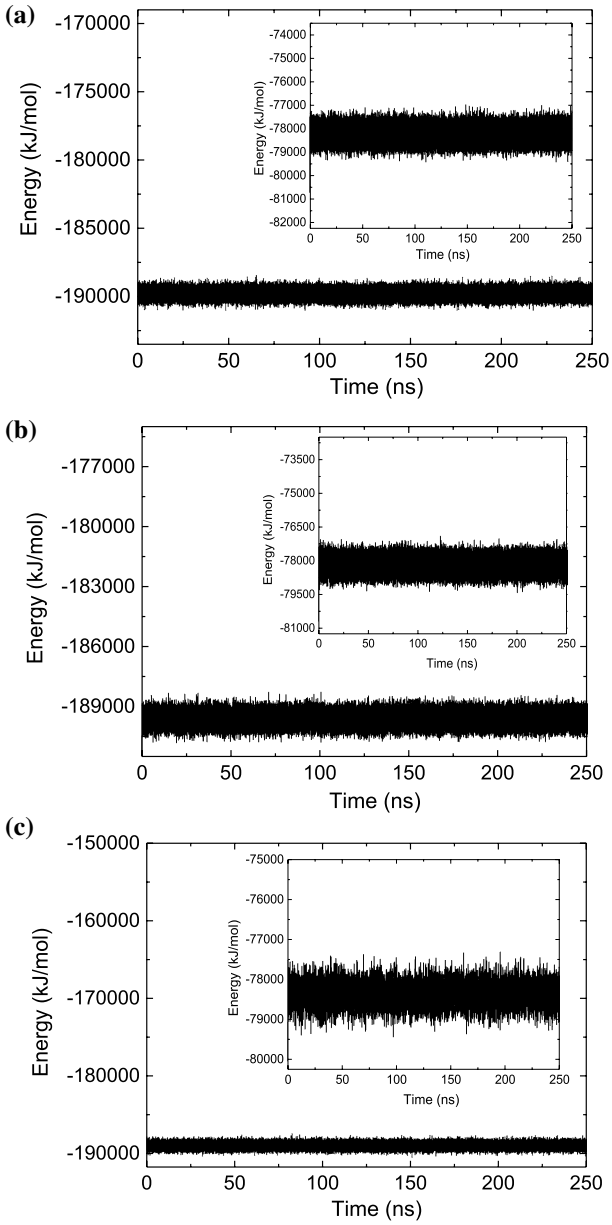

Fig. 3 From up to down three calculations at 310 K considering the potential energies for CDs immersed in RL solution (main panel) and water (inset): **a** α-CD, **b** β-CD, and **c** γ-CD

square deviation-RMSD relative to initial structure selecting 310 K (mammalian physiological temperature). This temperature was used as a representative illustration due to relevance for animal physiology and clinical applications.

The simulations revealed that all systems are energetically stable. However, due to the large number of conformations, which define the stability of biological systems, we observed fluctuations and a partial equilibrium regime, evidenced by many plateaus around average values for the α-CD, β-CD, and γ-CD complexes. It is important to mention that in both water and RL solution the γ-CD appears more stable than

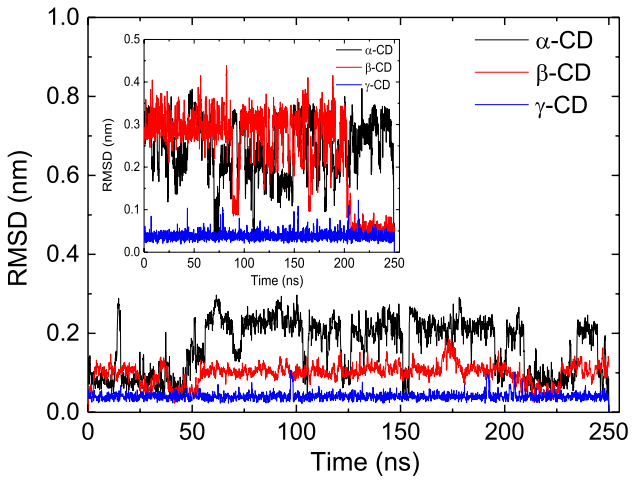

Fig. 4 A representative RMSD profile, taken at 310 K, considering CDs immersed in RL solution (main panel) and water (inset)

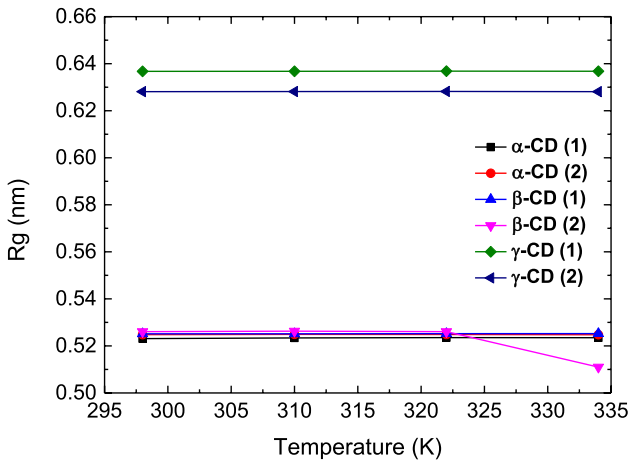

Fig. 5 The *Rg* profile of each CD as a function of the temperature. The numbers 1 and 2 in parentheses represent water and RL solution, respectively

α-CD and β-CD complexes. Figure 4 brings a representative view of RMSD in both solutions displaying the same equilibrium states as experimented by the systems. We also investigated the root mean square fluctuation (RMSF) value for all CD atoms concerning their initial coordinates. In this context, Figure S1 from Supplementary Material depicts the difference between the medium providing a more precise view of CD flexibility. The difference in CD fluctuations is much larger when the CBD binds in water as a solvent, perhaps related to structured waters near the complexes.

Temperature dependence of the radius of gyration (Rg), displayed in Fig. 5, indicates that in water the average values around 0.523 nm (α-CD), 0.528 nm (β-CD), and 0.638 nm (γ-CD) are close to those found in the RL solution. The only exception was computed for β-CD in the RL solution, where *Rg* decreased to 0.171 nm at 322 K, showing that Rg is not substantially affected by this solvent concentration or temperature in these simulations.

CBD displacement

The CBD retention time into CD for the temperature range assumed here may be directly linked to steric effects caused by the average displacement of the hydroxyl group atoms, especially in the saline medium. The retention time is short at high temperature for α-CD or β-CD and long for γ-CD because of the balance among non-bonded forces. The driving forces of complexation are non-bonded interactions acting among the CBD, cavity, and solvent (Tong and Wen 2008). In the present investigation, only the methyl group that bonded to the aromatic ring from CBD is encapsulated in the α-CD or β-CD, configuring a partial CBD-CD interaction, although, in some cases, CBD drifts to move large distances outwards from cavity. Snapshots at last frame of simulation (Figs. S2–S4, Supplementary Material) evidence that CBD occupies the wide side cavity of the CD, whereas its more flexible tail part tends to stick out toward the solvent. Furthermore, when CDB is partially inserted in CD it acquires distinct conformations. Defining the *z*-axis as the axis through of the CD center, the stretched initial orientation of the CBD is observed in the direction of the *y*-axis for 310 K (α-CD). In temperatures ranging 310–334 K, tail direction follows the y-axis for β-CD. An interesting result is the CD rotation (90º) in the RL solution; however, it does not change its conformation as response to CBD orientation that is free to rotate until leaving the CD cavity.

Numerous conformations above 310 K caused translation movement of the ligand out of the CD cavity (M1 movie in the Supplementary Material), allowing the entrance of other molecules into the cavity. This phenomenon occurs because non-bonded interactions are not sufficient to counterbalance the CBD configurational entropy increase as a response to the rising temperature. Specially, for RL solution, we evaluated translational movement measuring the distance between the CD and CBD centers. Between 310 and 334 K, the distance for β-CD increased from 0.248 to 0.526 nm, while for α-CD it changed from 0.248 to 0.481 nm, when temperature rises from 322 to 334 K. The γ-CD complex remains stable with restricted movement into the cavity for all temperatures, even when the wide side cavity showed to be occupied by cluster of lactate molecules and others ions.

We also documented, concerning α-CD and β-CD, a stronger interaction between lactate and γ-CD, such as a formation of lactate clusters (26 to 28 molecules, depending of temperature) around the CBD- γ-CD cavity as shown in the Supplementary Material (Figure S5). However, we did not find clusters formed among the ions. In early work, Silva and Santos 2018 have reported similar behavior between an

ionic solvent in the estradiol-sex hormone-binding globulin (SHBG) complex, suggesting the existence of an attractor at the SHBG surface (Da Silva and Dos Santos 2018). An inspection of electrostatic and van der Waals contributions, looking at the interaction between CDs and RL components (Tables 2, 3, 4), indicates that the average positioning of these components on CDs favor, in general, the prevalence of electrostatic interactions. However, this behavior changes with respect to lactate, where the attractive component of van der Waals dominates the interaction. The data reveal that temperature continuously changes the reorientation of the components of the RL solution in relation to the CD molecule due to the electrodynamics effect, producing an oscillating behavior of the interactions. Moreover, the results show that temperature continuously changes the reorientation of the components of the RL solution with the CD molecule due to the electrodynamics effect producing an oscillating behavior of the interactions. For example, for the Ca^{+2} interacting with α-CD, an increase in electrostatic attraction and the attractive component of van der Waals is observed for the temperature range from 298 to 310 K, but this attraction decreases at 322 K. It increases again at 334 K, while for K^+ the repulsive component of the van der Waals interaction continually rises when the temperature increases. Tables 5, 6, 7 show these interactions in respect to CBD and the components of the RL solution. The energies also maintain the oscillating pattern, with emphasis on the attractive component of van der Waals that dominates the lactate-CD interaction. Altogether, we conclude that there the unfavorable variation in electrostatic energy is compensated by the attractive component of van der Waals, where the balance between these interactions controls the binding energy. This result of the temperature action in the intermolecular interactions, when the CBD-CD complex is solvated in certain salt concentration, such as the dielectric constant is modified.

The calculations for HB, performed taking into account the distance from the donor atom and acceptor considering ≤ 0.35 nm and angle ≤ 30º, demonstrated that the amount of HB between CBD and CDs as a function of temperature has a stable number of interactions for β-CD (RL) and γ-CD (both solvents). We found an average of 0.1 bonds when the solvent is water, but no HB was found on γ-CD when the solution is RL, unlike β-CD whose mean HB was 0.9. In fact, on the α-CD, the number of HB increased from 0.15 (298 K) to 0.42 (322 K and 334 K), while in β-CD water it reduced from 0.25 HB (322 K) to 0.0 (334 K). Therefore, we credit the difference in the amount of HB formed between CBD-CD, not only to the increase in temperature, but also to the environment produced by the solvent. In water, the distance of ~ 0.2 nm between the centers of mass of the CBD and the γ-CD in relation to the temperature range studied, showed that the CBD is stable within the cavity, whereas for α-CD and β-CD the distance remains around 0.29 nm. On the other hand, in the RL solution, the CBD escapes from the β-CD when temperature greater than or equal to 310 K, whereas for α-CD the thermal threshold was at 322 K. In summary, this specific finding suggests that van der Waals interaction combined with hydrophobic contacts, play an important role in the γ-CD stabilization.

Effects of RL solution

The environment generated by the solvent affects the properties of interaction CBD-CD. The properties of the medium naturally depend on the component properties, such as size, charge, and the balance of interactions. The arrangements of solvent molecules around and inside the complexes are analyzed by calculating the radial distribution function $g(r)$ for the CDs centers. Relative to α-CD and β-CD, some molecules of water are located in the cavities for both solvents. At average, most water molecules are found at the narrow side of the cavities, when only water is the solvent, following the quantities: 2, 3 and 3.5 for α-CD, β-CD, and γ-CD, respectively. On the other hand, in the RL solution the average values for the number of water molecules are practically unaltered. Figure 6 presents a reduction in the number of solvent molecules (RL solution) from 310 K around the β-CD complex and few molecules remain inside the cavities. We also highlight the permanent presence of the one-lactate molecule in the cavity of the β-CD and about three water molecules inside γ-CD.

When the solvent is only water, the calculation indicates the existence of many water molecules around 0.8 nm from the CD center, corresponding to the more pronounced peak in the α-CD and β-CD complexes (data not shown). Nevertheless, in γ-CD the peak occurs at 0.2 nm and a second at 0.5 nm from the center. When analyzed in the RL solution, $g(r)$ gives a significant difference in the distribution of solvents, indicating that ions around the α-CD and β-CD tends to increase at 310 K reaching 0.80 and 0.72, respectively. Nevertheless, in several cases for the CBD-CD interaction, some water molecules remaining inside of the cavities. The temperature increasing promotes water loss from the cavity starting at 310 K, while hydration shells over CD become more mobile and diffuse into bulk water (Frank et al. 2002).

Binding free energy calculations

In this section, let us analyze the consequences of different solutions on binding free energy. Ions themselves seem to have large effects over complexation and stability of the complexes. It has been suggested that, in some cases, counterions participate directly in complex formation that is in the generation of a ternary drug-CD-salt (Kawabata et al. 2011). The data presented in Tables 5, 6, 7 give account

Table 2 Non-bonded energies between α-CD and RL solution components at a temperature ranging from 298 to 334 K

Temp (K)	Electrostatic (KJ/mol) Lenard Jones (KJ/mol)	Lactate	Ca^{+2}	K^+	Na^+	Cl^-	H_2O
298		$(-1558.73 \pm 2.97) \times 10^{-2}$	$(-.17 \pm 1.00) \times 10^{-3}$	$(-62.08 \pm 3.91) \times 10^{-3}$	$(-674.55 \pm 4.95) \times 10^{-2}$	$(-3720.12 \pm 9.24) \times 10^{-2}$	$(-2535.86 \pm 1.55) \times 10^{-1}$
		$(-7585.70 \pm 7.24) \times 10^{-2}$	$(-171.61 \pm 2.86) \times 10^{-4}$	$(25.69 \pm 1.39) \times 10^{-3}$	$(119.97 \pm 1.09) \times 10^{-2}$	$(-239.11 \pm 2.31) \times 10^{-2}$	$(-7589.05 \pm 6.27) \times 10^{-2}$
310		$(-1398.56 \pm 2.93) \times 10^{-2}$	$(-8.26 \pm 1.54) \times 10^{-3}$	$(-142.06 \pm 5.51) \times 10^{-3}$	$(-582.54 \pm 4.74) \times 10^{-2}$	$(-3432.65 \pm 8.99) \times 10^{-2}$	$(-2506.22 \pm 1.56) \times 10^{-2}$
		$(-6616.01 \pm 7.22) \times 10^{-2}$	$(-222.49 \pm 3.38) \times 10^{-4}$	$(48.89 \pm 2.00) \times 10^{-3}$	$(103.19 \pm .106) \times 10^{-2}$	$(-317.26 \pm 2.23) \times 10^{-2}$	$(-7880.24 \pm 6.19) \times 10^{-2}$
322		$(-1266.93 \pm 2.80) \times 10^{-2}$	$(-2.54 \pm 1.25) \times 10^{-3}$	$(-133.99 \pm 5.50) \times 10^{-3}$	$(-588.07 \pm 4.66) \times 10^{-2}$	$(-3234.76 \pm 8.83) \times 10^{-2}$	$(-2376.83 \pm 1.53) \times 10^{-1}$
		$(-6937.79 \pm 8.35) \times 10^{-2}$	$(-137.83 \pm 2.65) \times 10^{-4}$	$(53.99 \pm 2.03) \times 10^{-3}$	$(104.31 \pm 1.04) \times 10^{-2}$	$(-287.24 \pm 2.18) \times 10^{-2}$	$(-7538.28 \pm 6.43) \times 10^{-2}$
334		$(-989.39 \pm 2.82) \times 10^{-2}$	$(-24.27 \pm 2.04) \times 10^{-3}$	$(-152.58 \pm 5.79) \times 10^{-3}$	$(-732.80 \pm 4.93) \times 10^{-2}$	$(-3049.62 \pm 8.50) \times 10^{-2}$	$(-2443.28 \pm 1.59) \times 10^{-1}$
		$(-13{,}169.50 \pm 8.88) \times 10^{-2}$	$(-282.62 \pm 3.81) \times 10^{-4}$	$(55.24 \pm 2.10) \times 10^{-3}$	$(131.49 \pm 1.15) \times 10^{-2}$	$(-227.79 \pm 2.08) \times 10^{-2}$	$(-6367.84 \pm 6.14) \times 10^{-2}$

Table 3 Non-bonded energies between β-CD and RL solution components at a temperature ranging from 298 to 334 K

Temp (K)	Electrostatic (kJ/mol) Lenard Jones (kJ/mol)	Lactate	Ca^{+2}	K^+	Na^+	Cl^-	H_2O
298		$(-1165.66 \pm 2.93) \times 10^{-2}$	$(6.65 \pm 1.74) \times 10^{-3}$	$(-236.71 \pm 8.08) \times 10^{-3}$	$(-1780.35 \pm 7.80) \times 10^{-2}$	$(-1582.55 \pm 4.73) \times 10^{-2}$	$(-2673.32 \pm 1.47) \times 10^{-1}$
		$(-7518.30 \pm 8.80) \times 10^{-2}$	$(-319.76 \pm 3.94) \times 10^{-4}$	$(68.96 \pm 2.51) \times 10^{-3}$	$(312.05 \pm 1.73) \times 10^{-2}$	$(-621.51 \pm 1.37) \times 10^{-2}$	$(-7172.51 \pm 6.50) \times 10^{-2}$
310		$(-947.6 \pm 3.34) \times 10^{-2}$	$(-18.16 \pm 1.87) \times 10^{-3}$	$(-232.76 \pm 7.01) \times 10^{-3}$	$(-1747.54 \pm 7.96) \times 10^{-2}$	$(-1732.57 \pm 5.01) \times 10^{-2}$	$(-2683.67 \pm 1.40) \times 10^{-1}$
		$(-5998.30 \pm 6.97) \times 10^{-2}$	$(-285.18 \pm 3.93) \times 10^{-4}$	$(69.16 \pm 2.37) \times 10^{-3}$	$(307.58 \pm 1.77) \times 10^{-2}$	$(-643.03 \pm 1.49) \times 10^{-2}$	$(-7936.47 \pm 6.63) \times 10^{-2}$
322		$(-1553.32 \pm 3.34) \times 10^{-2}$	$(-25.94 \pm 1.59) \times 10^{-3}$	$(-254.94 \pm 8.12) \times 10^{-3}$	$(-1791.85 \pm 8.24) \times 10^{-2}$	$(-1653.36 \pm 5.02) \times 10^{-2}$	$(-2361.53 \pm 1.50) \times 10^{-1}$
		$(-1114.98 \pm 1.33) \times 10^{-1}$	$(-191.92 \pm 3.05) \times 10^{-4}$	$(72.98 \pm 2.53) \times 10^{-3}$	$(320.60 \pm 1.84) \times 10^{-2}$	$(-548.46 \pm 1.39) \times 10^{-2}$	$(-7019.40 \pm 6.55) \times 10^{-2}$
334		$(-1698.65 \pm 3.39) \times 10^{-2}$	$(-15.04 \pm 1.02) \times 10^{-3}$	$-133.98 \pm 5.38) \times 10^{-3}$	$(-1214.61 \pm 6.71) \times 10^{-2}$	$(-1974.65 \pm 6.17) \times 10^{-2}$	$(-2495.52 \pm 1.55) \times 10^{-1}$
		$(-11179.64 \pm 8.70) \times 10^{-2}$	$(-98.79 \pm 2.24) \times 10^{-4}$	$(46.57 \pm 1.87) \times 10^{-3}$	$(212.94 \pm 1.49) \times 10^{-2}$	$(-383.21 \pm 1.58) \times 10^{-2}$	$(-6026.44 \pm 6.44) \times 10^{-2}$

Table 4 Non-bonded energies between γ-CD and RL solution components at a temperature ranging from 298 to 334 K

Temp (K)	Electrostatic (kJ/mol) Lenard Jones (kJ/mol)	Lactate	Ca^{+2}	K^+	Na^+	Cl^-	H_2O
298		$(-2.1021.49 \pm 2.58) \times 10^{-}$	$(-125.13 \pm 6.95) \times 10^{-3}$	$(-49.14 \pm 1.00) \times 10^{-2}$	$(-371.06 \pm 1.07) \times 10^{-1}$	$(-2.4732.06 \pm 9.40) \times 10^{-}$	$(-6361.89 \pm 2.13) \times 10^{-1}$
		$(-2.6915.20 \pm 6.38) \times 10^{-}$	$(-143.14 \pm 9.12) \times 10^{-4}$	$(105.71 \pm 3.00) \times 10^{-3}$	$(560.92 \pm 2.29) \times 10^{-2}$	$(-588.54 \pm 2.65) \times 10^{-2}$	$(-4745.64 \pm 8.57) \times 10^{-2}$
310		$(-941.59 \pm 2.53) \times 10^{-2}$	$(-164.83 \pm 6.95) \times 10^{-3}$	$(-3.355.70 \pm 8.34) \times 10^{-}$	$(-340.65 \pm 1.02) \times 10^{-1}$	$(-2.3884.46 \pm 8.50) \times 10^{-}$	$(-6299.23 \pm 1.40) \times 10^{-1}$
		$(-2.7519.5\ 5 \pm 6.73) \times 10^{-}$	$(-441.58 \pm 7.69) \times 10^{-4}$	$(69.98 \pm 2.48) \times 10^{-3}$	$(499.96 \pm 2.17) \times 10^{-2}$	$(-504.37 \pm 2.46) \times 10^{-2}$	$(-4560.80 \pm 8.72) \times 10^{-2}$
322		$(-2.1151.60 \pm 2.73) \times 10^{-}$	$(-107.26 \pm 3.29) \times 10^{-3}$	$(-52.17 \pm 1.01) \times 10^{-2}$	$(-2910.88 \pm 9.34) \times 10^{-2}$	$(-2.3733.29 \pm 8.72) \times 10^{-}$	$(-6099.20 \pm 2.08) \times 10^{-1}$
		$(-2.7760.57 \pm 6.42) \times 10^{-}$	$(-461.56 \pm 6.18) \times 10^{-4}$	$(106.80 \pm 2.96) \times 10^{-3}$	$(416.28 \pm 1.96) \times 10^{-2}$	$(-293.55 \pm 2.43) \times 10^{-2}$	$(-4563.69 \pm 8.66) \times 10^{-2}$
334		$(-947.11 \pm 2.49) \times 10^{-2}$	$(-137.8\ 6 \pm 3.25) \times 10^{-3}$	$(-3.333.45 \pm 8.07) \times 10^{-}$	$(-2906.19 \pm 9.48) \times 10^{-2}$	$(-2.3570.93 \pm 8.41) \times 10^{-}$	$(-5938.72 \pm 2.07) \times 10^{-1}$
		$(-2.7438.57 \pm 6.73) \times 10^{-}$	$(-342.28 \pm 4.73) \times 10^{-4}$	$(69.39 \pm 2.44) \times 10^{-3}$	$(427.45 \pm 2.04) \times 10^{-2}$	$(-439.40 \pm 2.40) \times 10^{-2}$	$(-4475.62 \pm 8.68) \times 10^{-2}$

Table 5 Non-bonded energies between CBD (encapsulated in the α-CD) and RL solution components at a temperature ranging from 298 to 334 K

Temp (K)	Electrostatic (kJ/mol) Lenard Jones (kJ/mol)	Lactate	Ca^{+2}	K^+	Na^+	Cl^-	H_2O
298		$(905.23 \pm 9.63) \times 10^{-3}$	$(123.58 \pm 4.88) \times 10^{-4}$	$(42.96 \pm 1.09) \times 10^{-3}$	$(91.23 \pm 2.42) \times 10^{-2}$	$(-470.90 \pm 2.00) \times 10^{-2}$	$(-9819.34 \pm 7.33) \times 10^{-2}$
		$(-9392.72 \pm 6.19) \times 10^{-2}$	$(-72.65 \pm 2.09) \times 10^{-4}$	$(-7.87 \pm 2.76) \times 10^{-4}$	$(10.89 \pm 6.71) \times 10^{-3}$	$(-2014.98 \pm 6.25) \times 10^{-3}$	$(-3761.18 \pm 4.20) \times 10^{-2}$
310		$(42.05 \pm 1.20) \times 10^{-2}$	$(44.37 \pm 4.08) \times 10^{-4}$	$(216.01 \pm 6.85) \times 10^{-4}$	$(-736.62 \pm 7.41) \times 10^{-2}$	$(-473.03 \pm 2.01) \times 10^{-2}$	$(-8440.72 \pm 8.64) \times 10^{-2}$
		$(-2.9910.65 \pm 7.02) \times 10^{-}$	$(-51.31 \pm 2.29) \times 10^{-4}$	$(-9.07 \pm 1.70) \times 10^{-4}$	$(220.23 \pm 2.14) \times 10^{-2}$	$(-1817.29 \pm 6.47) \times 10^{-3}$	$(-3314.01 \pm 4.42) \times 10^{-2}$
322		$(104.92 \pm 1.06) \times 10^{-2}$	$(150.82 \pm 4.49) \times 10^{-4}$	$(38.56 \pm 1.09) \times 10^{-2}$	$(1316.42 \pm 7.45) \times 10^{-3}$	$(-406.58 \pm 1.93) \times 10^{-2}$	$(-8617.27 \pm 7.88) \times 10^{-2}$
		$(-2.9368.27 \pm 6.90) \times 10^{-}$	$(-112.18 \pm 2.52) \times 10^{-4}$	$(-4.75 \pm 3.25) \times 10^{-4}$	$(-1577.76 \pm 6.83) \times 10^{-4}$	$(-1602.06 \pm 5.98) \times 10^{-3}$	$(-3202.19 \pm 4.61) \times 10^{-2}$
334		$(102.10 \pm 1.27) \times 10^{-2}$	$(90.18 \pm 4.27) \times 10^{-4}$	$(257.19 \pm 9.00) \times 10^{-4}$	$(-230.33 \pm 1.12) \times 10^{-1}$	$(-584.89 \pm 2.16) \times 10^{-2}$	$(-6508.31 \pm 9.71) \times 10^{-2}$
		$(-2.11416.39 \pm 8.29) \times 10^{-}$	$(-49.34 \pm 1.45) \times 10^{-4}$	$(-8.51 \pm 2.18) \times 10^{-4}$	$(636.79 \pm 3.27) \times 10^{-2}$	$(-2609.02 \pm 7.89) \times 10^{-3}$	$(-4216.27 \pm 4.56) \times 10^{-2}$

Table 6 Non-bonded energies between CBD (encapsulated in the β-CD) and RL solution components at a temperature ranging from 298 to 334 K

Temp (K)	Electrostatic (kJ/mol) Lenard Jones (kJ/mol)	Lactate	Ca^{+2}	K^+	Na^+	Cl^-	H_2O
298		$(12.81 \pm 1.08) \times 10^{-2}$	$(72.39 \pm 2.24) \times 10^{-4}$	$(20.00 \pm 1.03) \times 10^{-3}$	$(88.02 \pm 1.37) \times 10^{-2}$	$(-262.22 \pm 1.32) \times 10^{-2}$	$(-10439.10 \pm 6.94) \times 10^{-2}$
		$(-8265.90 \pm 9.16) \times 10^{-2}$	$(-62.19 \pm 1.28) \times 10^{-4}$	$(1.47 \pm 4.52) \times 10^{-4}$	$(-116.38 \pm 3.54) \times 10^{-3}$	$(-2519.56 \pm 6.23) \times 10^{-3}$	$(-4481.67 \pm 5.38) \times 10^{-2}$
310		$(-88.33 \pm 1.50) \times 10^{-2}$	$(17.91 \pm 2.38) \times 10^{-4}$	$(216.61 \pm 9.94) \times 10^{-4}$	$(1026.14 \pm 7.03) \times 10^{-3}$	$(-270.91 \pm 1.43) \times 10^{-2}$	$(-9198.02 \pm 7.14) \times 10^{-2}$
		$(-9354.18 \pm 8.07) \times 10^{-2}$	$(-32.01 \pm 1.34) \times 10^{-4}$	$(-.59 \pm 3.09) \times 10^{-4}$	$(-169.70 \pm 1.13) \times 10^{-3}$	$(-2147.57 \pm 5.78) \times 10^{-3}$	$(-3912.56 \pm 4.70) \times 10^{-2}$
322		$(-83.06 \pm 1.45) \times 10^{-2}$	$(74.52 \pm 3.61) \times 10^{-4}$	$(230.57 \pm 9.00) \times 10^{-4}$	$(-366.10 \pm 1.40) \times 10^{-1}$	$(-385.04 \pm 1.71) \times 10^{-2}$	$(-583.67 \pm 1.11) \times 10^{-1}$
		$(-10599.32 \pm 8.52) \times 10^{-2}$	$(-46.36 \pm 1.31) \times 10^{-4}$	$(-12.34 \pm 2.35) \times 10^{-4}$	$(866.45 \pm 3.65) \times 10^{-2}$	$(-3012.57 \pm 7.54) \times 10^{-3}$	$(-4767.91 \pm 4.93) \times 10^{-2}$
334		$(55.01 \pm 1.42) \times 10^{-2}$	$(118.24 \pm 3.82) \times 10^{-4}$	$(321.85 \pm 9.45) \times 10^{-4}$	$(-41.98 \pm 3.20) \times 10^{-2}$	$(-538.11 \pm 1.19) \times 10^{-2}$	$(-9189.16 \pm 8.77) \times 10^{-2}$
		$(-11723.81 \pm 8.00) \times 10^{-2}$	$(-100.65 \pm 2.44) \times 10^{-4}$	$(-1.20 \pm 2.86) \times 10^{-4}$	$(296.37 \pm 9.68) \times 10^{-3}$	$(-2346.73 \pm 7.44) \times 10^{-3}$	$(-4344.98 \pm 5.11) \times 10^{-2}$

Table 7 Non-bonded energies between CBD (encapsulated in the γ-CD) and RL solution components at a temperature ranging from 298 to 334 K

Temp (K)	Electrostatic (kJ/mol) Lenard Jones (kJ/mol)	Lactate	Ca^{+2}	K^+	Na^+	Cl^-	H_2O
298		$(-675.48 \pm 9.58) \times 10^{-3}$	$(106.05 \pm 3.69) \times 10^{-4}$	$(210.60 \pm 4.98) \times 10^{-4}$	$(831.82 \pm 3.45) \times 10^{-3}$	$(-861.28 \pm 3.61) \times 10^{-3}$	$(-2715.64 \pm 5.32) \times 10^{-2}$
		$(-5041.91 \pm 3.14) \times 10^{-2}$	$(-38.88 \pm 1.08) \times 10^{-4}$	$(-115.27 \pm 8.48) \times 10^{-5}$	$(-898.70 \pm 3.45) \times 10^{-4}$	$(-953.07 \pm 2.72) \times 10^{-3}$	$(-2365.83 \pm 2.29) \times 10^{-2}$
310		$(-1048.20 \pm 9.69) \times 10^{-3}$	$(53.48 \pm 2.80) \times 10^{-4}$	$(187.23 \pm 4.99) \times 10^{-4}$	$(649.83 \pm 4.62) \times 10^{-3}$	$(-545.91 \pm 2.72) \times 10^{-3}$	$(-3004.58 \pm 4.99) \times 10^{-2}$
		$(-4970.59 \pm 3.32) \times 10^{-2}$	$(-209.42 \pm 8.10) \times 10^{-5}$	$(-5.05 \pm 1.49) \times 10^{-4}$	$(-713.34 \pm 7.71) \times 10^{-4}$	$(-700.37 \pm 2.31) \times 10^{-3}$	$(-2321.15 \pm 2.37) \times 10^{-2}$
322		$(-1061.20 \pm 9.51) \times 10^{-3}$	$(141.67 \pm 4.83) \times 10^{-4}$	$(129.91 \pm 3.91) \times 10^{-4}$	$(653.02 \pm 3.75) \times 10^{-3}$	$(-509.68 \pm 2.83) \times 10^{-3}$	$(-2986.59 \pm 4.86) \times 10^{-2}$
		$(-4761.77 \pm 3.75) \times 10^{-2}$	$(-48.48 \pm 1.48) \times 10^{-4}$	$(-74.93 \pm 8.38) \times 10^{-5}$	$(-726.17 \pm 6.08) \times 10^{-4}$	$(-668.38 \pm 2.27) \times 10^{-3}$	$(-2350.45 \pm 2.57) \times 10^{-2}$
334		$(-643.83 \pm 9.11) \times 10^{-3}$	$(169.20 \pm 8.46) \times 10^{-5}$	$(134.61 \pm 4.32) \times 10^{-4}$	$(683.75 \pm 3.90) \times 10^{-3}$	$(-564.63 \pm 3.08) \times 10^{-3}$	$(-2657.53 \pm 5.20) \times 10^{-2}$
		$(-4436.13 \pm 3.60) \times 10^{-2}$	$(-99.29 \pm 3.05) \times 10^{-5}$	$(-6.38 \pm 1.00) \times 10^{-4}$	$(-749.14 \pm 7.52) \times 10^{-4}$	$(-700.73 \pm 2.41) \times 10^{-3}$	$(-2349.03 \pm 2.49) \times 10^{-2}$

of the ionic effect over binding CBD-CD. Electrostatic and van der Waals interactions among CDB, CD, and ions can indicate, in terms of these interactions, an apparent formation of weak ternary complexes CBD-CD-Cl^- and CBD-CD-LAC, among others possible complexes. Still, according to Tables 5, 6, 7, it is suggested that there is a formation of CBD- α-CD-LAC > CBD- β-CD-LAC > CBD-γ-CD-LAC complexes in the same manner that CBD-β-CD-Cl^- < CBD-α-CD-Cl^- < CBD-γ-CD-Cl^-. When the salt dissolves, the counterions create a favorable pH change in the diffusion layer formed on the surface of the dissolving particle (Serajuddin 2007; Kawabata et al. 2011). The diffusion coefficient was calculated at 310 K between 10 and 150 ns of trajectory to ensure the mean number of ions are in bulk solvent (Supplementary Material, Table S3). The Na^+ mobility is higher than Cl^- because the first provides less attraction over water molecules than the latter, facilitating Na^+ motion in the solution. Figure 7 depicts the ion charge densities at box coordinates at 310 K, where the charge density oscillation is damping of electric fields caused by the presence of mobile ions. When the ion moves, there is a perturbation of the electrodynamics equilibrium, but the electric field produced by the ions themselves tends to restore the equilibrium. The average densities over CBD-CD complexes are the same: − 1.81 e nm^{-3} (Cl^-) and 1.71 e nm^{-3} (Na^+) for α-CD, β-CD, and γ-CD, showing a standard deviation of only ± 0.04 e nm^{-3}.

The binding free energy is expected to depend on salt concentration because of its action on the configurational entropy. Calculations of configurational entropy displayed lower changes in aqueous than in the RL solution. The CBD-CD binding directly undergoes influence of the changes in its conformations. From water to RL solution at 310 K, conformational entropy changes for CBD-α-CD: from 1070.83 to 1125.85 J/mol K; CBD-β-CD: from 1097.94 to 1310.59 J/mol K; CBD-γ-CD: from 715.95 to 854.52 J/mol K. The values were calculated using the quasi-harmonic method and the bias in the entropy from the water to the RL solution is consistent with binding, including CBD-γ-CD, due to greatest conformational restriction upon CBD, but also due to flexibility of the γ-CD, as we can verify in M2 movie available in the Supplementary Material.

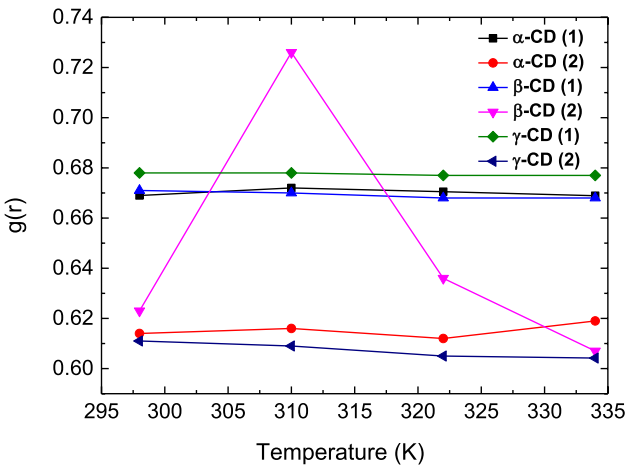

Fig. 6 The $g(r)$ behavior in relation to temperature. The numbers 1 and 2 in parentheses represent water and RL solution, respectively

In order to predict the binding free energies, the MM-PBSA approach was employed to estimate the binding free energies from 298 to 334 K, taking into account changes in conformational entropy. A value of $\varepsilon = 3$ was assumed as default for the internal dielectric constant, while the external dielectric constant was calculated with the GROMACS tool for each temperature as shown in Fig. 8. As shown in Fig. 9, further calculations exhibited the values of binding free energy as a function of temperature at the last 200 ns of simulation for each system. The results suggest that the salt effect on binding is a cause of the interactions declining between CBD and CD, when compared with the water medium. Consequently, the CBD-CD complexation must be less favorable when it is assumed in the RL solution instead of only in water solution. It is relevant to mention that the van der Waals interaction was the strongest contribution to CBD and CDs complexation. Yet, the results suggest that the entropy contribution is relevant for CBD-α-CD and CBD-β-CD, while CBD-γ-CD is practically insensitive to temperature for both solutions. It is interesting to note that the values of binding free energy at 322 K, produce complexes more stable than at room temperature, with the exception of CBD-α-CD (− 30.89 kJ mol^{-1} for 322 K and − 37.58 kJ mol^{-1} for 298 K) in water solution at room temperature. Considering the non-covalent interactions, one would expect a stability deterioration of the complexes as the temperature increases. At elevated thermal levels, water molecules inside the CD cavity are not energetically comparable to water molecules in the bulk (Buschmann et al. 2000).

We observed that enough water molecules escape from cavities at 322 K, except for the ones firmly bonded. The water molecule flux increases from the cavity towards CDs outside the hydrophobic contacts between atoms inner CDs cavity and CBD methyl group making binding more favorable. As a result, it seems that the ability of CD to enclose molecules is related to the cavity size, ligands dimension, temperature, and medium. The CD type plays an important role in the complexation of CBD-CD as we can see in α-CD, β-CD, and γ-CD complexes. It is important to mention that CD and drug-CD complexes do not easily cross biological membranes (Stella and He 2008). This could represent a potential pharmacological limitation, since the drug needs to be safely transported to the binding site, where it will be released from the complex. In this context, experiments have shown that only negligible amounts of hydrophilic CBD and

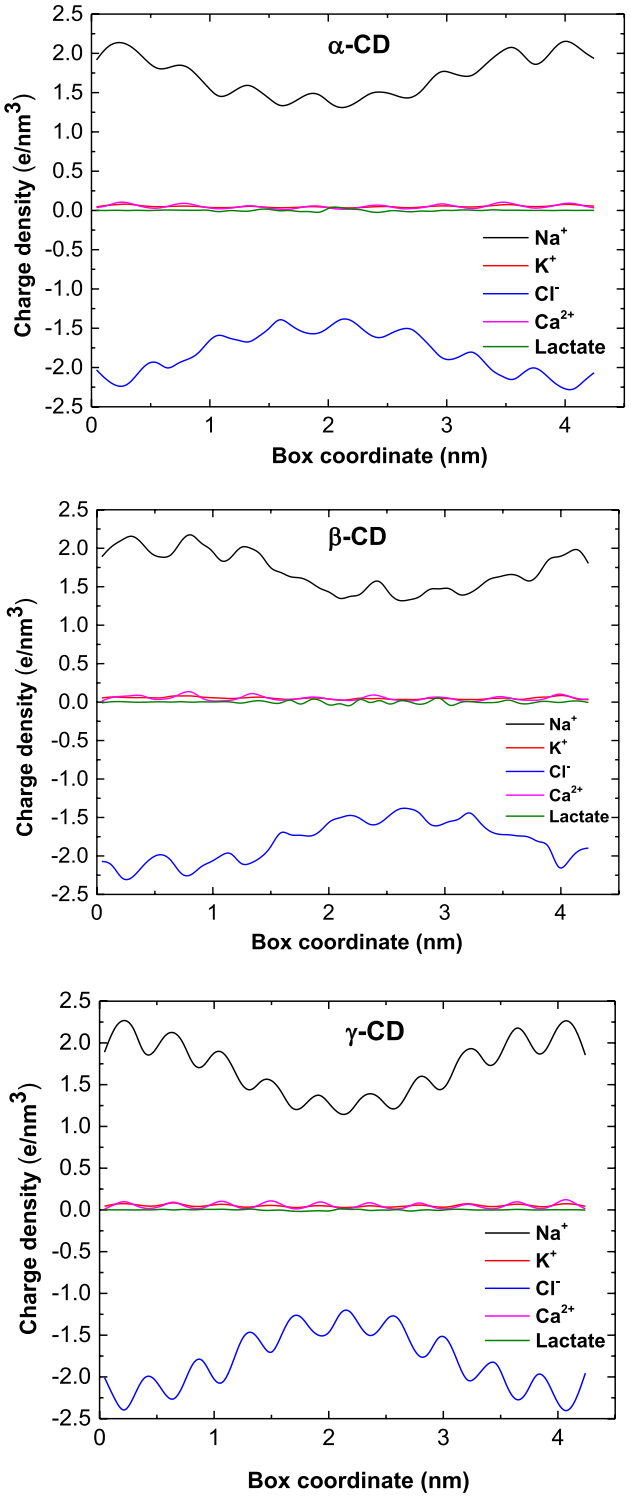

Fig. 7 Spectrum of charge density oscillation of RL solution components for each CD taken at 310 K

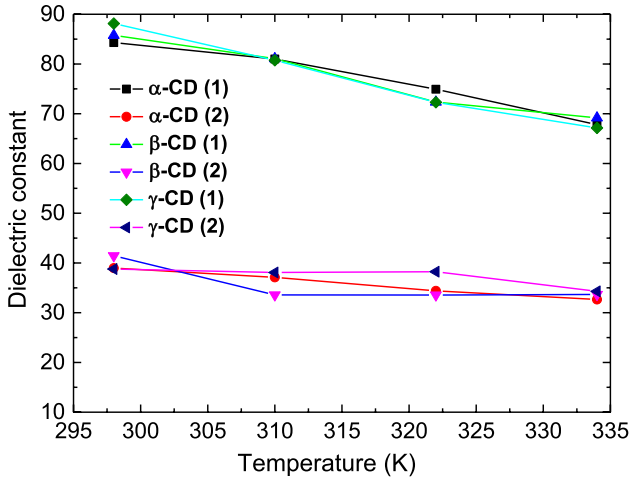

Fig. 8 External dielectric constant values concerning temperature. The numbers 1 and 2 in parentheses represent water and RL solution, respectively

drug-CD complexes can permeate lipophilic membranes such as those that compose the skin and gastrointestinal mucosa (Vazquez et al. 1991; Uekama et al. 1998). Therefore, in the cases where the CBD is partially encapsulated, due to its high lipophilicity the diffusion must be enhanced through the membrane (Fasinu et al. 2016; Ohlsson et al. 1986).

Further remarks

An important issue in pharmacy is how to preserve the stability of temperature-controlled pharmaceuticals without modifying their efficacy (Ziance et al. 2009). For example, ideally physiological solutions should maintain stability within a recommended temperature, established by the manufacturer. However, solutions are exposed during transport and storage to thermal gradient temperatures before they are administered to the patients. Thus, it is important to investigate possible temperature effects in the physical-chemistry properties of artificial physiological solutions. Motivated by clinical arguments the present investigation outlined the energetic behavior and possible biophysical role of the RL constituents regarding the inclusion mechanism of CBD within different CDs. Additionally, we opted to select different CDs, submitted to different thermal levels, because this strategy certainly allows for a better comprehension of both physiological and pharmacological aspects about the formation of the CDs-CBD complex.

In pharmacology, CDs applications require a precise understanding of the physiological scenario involved when these substances permeate the intestinal barrier and the blood–brain barrier (BBB) (Matsuda 1999; Vecsernyés et al. 2014). Understanding both interactions certainly could shed light on the potential side effects and how the drug-CD complex obtain access to the circulation and the central nervous system, where it will be transported toward the binding

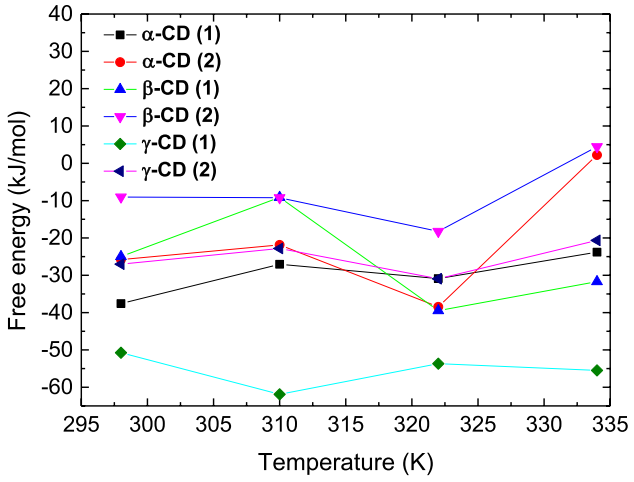

Fig. 9 Binding free energy of CBD-CD in relation to temperature. The numbers 1 and 2 in parentheses represent water and RL solution, respectively

site. Studies suggest that CDs intracerebral injections are associated with a certain level of toxicity, after its administration. Congruent with this finding, Vecsernyés et al. state that assumption of different CDs may be necessary due to the different degrees of toxicity imposed as result of interaction with the physiological substrate (Vecsernyés et al. 2014). Within this concern, Dreyfuss and Oppenheimer also presented a discussion on cellular interactions with CDs showing their effects on mammalian cells of endocrine, cardiovascular, immune, and nervous systems, among others (Dreyfuss and Oppenheimer 2011). According to these authors, the cellular effects are mostly based on CDs interplay with the cell membrane, rich in cholesterol and sphingolipids. In this context, CDs may remove cholesterol from the cellular membrane. Thus, such arguments must be considered if one considers CBDs therapeutic potential in several neurological diseases, such as epilepsy and brain tumors.

On the other hand, toxicological research has shown that γ-CD seems to be safe even when administered parenterally, while α-CD and β-CD are not suitable for this purpose. Injection of γ-CD promoted insignificant irritation, being rapidly degraded to glucose in the upper intestinal tract by intestinal enzymes (Valle 2004). Moreover, Monnaert et al. (2004) found that α-CD removed phospholipids and that β-CD extracted cholesterol and phospholipids from BBB membranes. Still according to these investigators, γ-CD was less lipid selective than the other CDs, implying a safer clinical application. These arguments, in conjunction with our results, in principle support γ-CD adoption as the more suitable candidate for CBD encapsulation and clinical application. Thus, the complex scenario pointed out by these works reinforced our strategy to consider different CDs-CBD interactions in the RL solution.

Our simulations showed that CBD is partially enveloped in α-CD and β-CD, while γ-CD fully engulfs the cannabinoid. Thus, to obtain efficient delivery from CDs, it is pertinent to understand a possible physiological scenario of CBD encapsulation degree within the CDs. This issue is particularly important if one reason is to understand how the interaction between CBD and the binding site could be affected by partial or even full encapsulation. The enveloping degree of CBD is even more pertinent since the level of encapsulation may be directly linked to the physicochemical properties of the host and guest molecules. Certainly, partial or total encapsulation may modulate the facility for releasing, when the complex achieves the binding site. In this framework, the level of CBD adjustment within CDs can also affect the level for a controlled release, hence it depends on the interactive forces between CD and CBD. In this sense, an intriguing question formulated by Stella asked how the CD is released if a drug is tightly bound to it (Stella and He 2008). Based on his questioning the partial encapsulation observed in our work may reflect that the forces that maintain the complex stable are weakening. In contrast, in total CBD enveloping such forces may have a greater magnitude. As we observed for CBD-γ-CD, full encapsulation may be beneficial for providing an electrostatic protection from the aqueous ambient and decrease an eventual toxicity level and side effects. Our results showed that the CBD total encapsulation may be clinically attractive thanks to the greater stability at all temperatures adopted here (in particular with respect to the physiological framework), which could guarantee a controlled release of cannabinoid. Nevertheless, since CBD is a non-intoxicating cannabinoid, both α-CD and β-CD, in which they formed a partial encapsulation, also arise as a secondary pharmacological option. Partial encapsulation could facilitate the release of CBD over the binding site compared to the total encapsulation. Conversely, partial encapsulation can decrease the CBD-CD complex stability, making it more difficult to have a controlled release of the cannabinoid. Summarizing, although our investigation suggests that γ-CD represents the best choice, the pros and cons presented here depict a complex scenario, emphasizing the necessity for additional theoretical and experimental investigations.

The present report also characterized how aqueous solutions interact with the CBD and CDs as well as the CBD-CDs complex itself in different thermal conditions. To make an approximation with an artificial physiological environment, it was important to consider the physiological temperature, such as a saline fluid constituted by components found in the mammal plasma. This strategy allowed us to determine the magnitude of the specific energies of the interaction of each ionic species and the lactate molecule with the

CD and CBD. The simulations provided a more pronounced energy interaction between all CDs with water, lactate, and Cl^-. Despite of the hydrophobic nature of CBD, it is also important to identify which solute component interacts more intensely with this cannabinoid, especially if one considers that α-CD and β-CD were observed to be partially encapsulated. In this context, a theoretical study is also convenient to understand the CBD interaction with RL solution components as a function of temperature. The energetic analysis revealed that CBD interacts more intensely with water, lactate, and Cl^- no matter the temperature value. The lack of explicit functional thermic dependence on the energy magnitude may be credited to water activity influence on the dielectric constant and complex electrostatic screening effects promoted by clustering such as ion-water and ion-ion interactions (Sipahiolgu et al. 2003; Chandra 2000; Li et al. 2017). In this sense, the distinct levels of attractions and repulsion forces presented in Tables 2, 3, and 4 could be a consequence of dynamics effects on the dielectric constant, mediated by water and different ions species and their concentrations, respectively.

According to our findings, at physiological temperature, the kinetic and potential energies exhibit similar values and temporal stability for the three CDs. However, if one inspects the RMSD and RMSF it is possible to observe fluctuations, especially pronounced when α-CD and β-CD are immersed in the RL solution. In contrast, γ-CD remains stable during the simulation, again emerging as a coherent option to encapsulate CBD. From the *Rg* and *g*(*r*) results, we also confirmed the γ-CD stability pattern no matter the thermal level used in the simulation. In summary, in conjunction with the previous discussion given above, these calculations also emphasized that the thermal paradigm used here, did not impose measurable changes in the structural flexibility. In other words, RMSD and RMSF calculations did not show a stability reduction of the system formed by the γ-CD-CBD complex. In this sense, γ-CD is the best choice for clinical purposes, where the RL solution containing the complex, could be prepared at a physiological temperature before administration. Surely, this empirical procedure could provide more stability a priori, by minimizing undesirable fluctuations, which could affect the encapsulation performance and controlled CBD release. It is worth mentioning that stabilization between CBD-CDs was reinforced, thanks to the fact that the number of hydrogen bonds does not significantly change during the simulation.

The results extracted CBD-γ-CD reinforced a particular attention only on this system. We observe lactate clusters in front of the γ-CD cavity, without a dramatic thermal modulation of the number of lactate molecules. Within this study temperature range, the number of hydrogen bonds practically does not increase between CBD and the four CDs as a function of the temperature. Finally, in contrast with the preferential orientation computed from the glucose cluster formation reported in our previous work, lactate did not exhibit any orientational preference for the four temperatures. Indeed, besides enhancing the stabilization, lactate clustering near CDs arises as a beneficial mechanism by preventing the lactic acidosis state (Da Silva and Dos Santos 2018; Goodwin et al. 2007; Nimmo et al.1991). In this scheme, as similarly observed in other systems, lactate assembly also may regulate protein conformational CBD-CDs stability in response to external perturbations (Imamura et al. 2003; Arakawa and Timasheff 1982). Last, but not least, lactate self-assembly emerges as a general mechanism for conformational stability enhancement of CDs against temperature changes. On the other hand, deleterious effects of lactate crowding on CDs are not discarded. Thus, this complex scenario configures the opportunity for deeper investigation on the lactate concentration influence on CDs. In this perspective, it is relevant to uncover the critical lactate concentration would represent the maximal limit between either beneficial or deleterious effects.

Conclusion

Summarizing, we can conclude that this research contributes to elucidating the energetic aspects related to the CBD-CDs interactions in water and a saline environment. Our results showed that the entropy contribution was relevant for CBD-α-CD and CBD-β-CD, while CBD-γ-CD remained practically thermally insensible in both aqueous environments. The γ-CD was the more stable complex when immersed in both water and the RL solution. Additionally, independently of the system temperature, CBD was partially encapsulated in α-CD and β-CD, whereas the cannabinoid is fully engulfed in γ-CD for both water and the RL solution. From a pharmacological point of view, γ-CD arises as the most appropriate host for CBD. On the other hand, α-CD and β-CD, although they pharmacologically do not represent the best option for encapsulation, the physiological relevance of each CD used here could be matter of further investigation for verifying our hypothesis about facilitation of CBD release at the binding site. Thus, further studies verifying in detail the physiological properties of each CD are required as well. The simulations also quantified the energetic aspects of the water and RL solution interaction with CDs and CBD, highlighting a remarkable interaction energy between lactate and CDs surface. In addition, movement of lactate components toward CDs also promoted clustering around this molecule. It could be interesting to investigate the lactate cluster regulation for both ionic concentrations and pH changes in the future. Finally, to achieve a more realistic physiological

scope, studies considering salt concentrations completely compatible with those found on RL solution are welcome.

Acknowledgements We would like to thank Dr. B. Piechocinska for careful reading of the manuscript and constructive remarks.

Compliance with ethical standards

Conflict of interest The authors declare that there is no conflict of interest.

References

Abraham MJ, van der Spoel D, Lindahl E, Hess B (2016) GROMACS User Manual Version 5.1. 2. GROMACS Development Team

Ameri A (1999) The effects of cannabinoids on the brain. Prog Neurobiol 58:315–348. https://doi.org/10.1016/s0301-0082(98)00087-2

Andersen P, Moser EI (1995) Brain temperature and hippocampal function. Hippocampus 5:491–498. https://doi.org/10.1002/hipo.450050602

Arakawa T, Timasheff SN (1982) Stabilization of protein structure by sugars. Biochemistry 21:6536–6544. https://doi.org/10.1021/bi00268a033

Baron EP (2015) Comprehensive review of medicinal marijuana, cannabinoids, and therapeutic implications in medicine and headache: what a long strange trip it's been…. Headache 55:885–916. https://doi.org/10.1111/head.12570

Baskett TF (2003) Sydney ringer and lactated ringer's solution. Resuscitation 58:5–7. https://doi.org/10.1016/s0300-9572(03)00209-0

Berendsen HJ, Postma JPM, van Gunsteren WF, DiNola AR, Haak JR (1984) Molecular dynamics with coupling to an external bath. J Chem Phys 81:3684–3690. https://doi.org/10.1063/1.448118

Bikkina SW, Bhati AG, Padhi SI, Priyakumar UD (2017) Temperature dependence of the stability of ion pair interactions, and its implications on the thermostability of proteins from thermophiles. J Chem Sci 129:405–414. https://doi.org/10.1007/s12039-017-1231-4

Bondoli A, Scrascia E, Magalini SI, Barbi S, Rocchi C, Cavaliere F (1978) Intravenous sodium lactate administration in respiratory alkalosis secondary to severe brain injuries. Resuscitation 6:279–284. https://doi.org/10.1016/0300-9572(78)90009-6

Brooks VB (1983) Study of brain function by local, reversible cooling. Rev Physiol Biochem Pharmacol 95:1–109. https://doi.org/10.1007/BFb0034097

Burstein S (2015) (CBD) and its analogs: a review of their effects on inflammation. Bioorg Med Chem 23:1377–1385. https://doi.org/10.1016/j.bmc.2015.01.059

Buschmann HJ, Dong H, Schollmeyer E (2000) Complexation of aliphatic alcohols by α- and β-cyclodextrin and their partial ethylated derivatives in aqueous solution. J Therm Anal Calorim 61:23–28. https://doi.org/10.1023/A:1010140019557

Cai W, Xia B, Shao X, Guo Q, Maigret B, Pan Z (2001) Molecular docking of α-cyclodextrin inclusion complexes by genetic algorithm and empirical binding free energy function. Chem Phys Lett 342:387–396. https://doi.org/10.1016/S0009-2614(01)00594-2

Chandra A (2000) Static dielectric constant of aqueous electrolyte solutions: is there any dynamic contribution? J Chem Phys 113:903–905. https://doi.org/10.1063/1.481870

Chaudhuri S, Chakraborty S, Sengupta PK (2010) Encapsulation of serotonin in β-cyclodextrin nano-cavities: fluorescence spectroscopic and molecular modelling studies. J Mol Struct 975:160–165. https://doi.org/10.1016/j.molstruc.2010.04.014428290

Chen P, Yao S, Chen X, Huang Y, Song H (2019) A new strategy for constructing the β-cyclodextrin-based magnetic nano-carriers: molecule docking technique. New J Chem 43:4282–4290. https://doi.org/10.1039/C8NJ06131A

Chevaleyre V, Takahashi KA, Castillo PE (2006) Endocannabinoid-mediated synaptic plasticity in the CNS. Annu Rev Neurosci 29:37–76. https://doi.org/10.1146/annurev.neuro.29.051605.112834

Chiang PC, Shi Y, Cui Y (2014) Temperature dependence of the complexation mechanism of celecoxib and hydroxyl-β-cyclodextrin in aqueous solution. Pharmaceutics 13:467–480. https://doi.org/10.3390/pharmaceutics6030467

Chung H, Fierro A, Pessoa-Mahana CD (2019) Cannabidiol binding and negative allosteric modulation at the cannabinoid type 1 receptor in the presence of delta-9-tetrahydrocannabinol: an in Silico study. PLoS ONE 14(7):e0220025. https://doi.org/10.1371/journal.pone.0220025

Da Silva AJ, Dos Santos ES (2018) Aqueous solution interactions with sex hormone-binding globulin and estradiol: a theoretical investigation. J Biol Phys 44:539–556. https://doi.org/10.1007/s10867-018-9505-8

Darden T, York D, Pedersen L (1993) Particle mesh Ewald: an N· log (N) method for Ewald sums in large systems. J Chem Phys 98:10089–10092. https://doi.org/10.1063/1.464397

DeLano WL (2011) The PyMOL molecular graphics system (Version 1.4. 1). DeLano Scientific LLC, San Carlos

Devane W, Hanus L, Breuer A, Pertwee R, Stevenson L, Griffin G, Mechoulam R (1992) Isolation and structure of a brain constituent that binds to the cannabinoid receptor. Science 258:1946–1949. https://doi.org/10.1126/science.1470919

Dodda LS, Cabeza de Vaca I, Tirado-Rives J, Jorgensen WL (2017) LigParGen web server: an automatic OPLS-AA parameter generator for organic ligands. Nucleic Acids Res 45:W331–W336. https://doi.org/10.1093/nar/gkx312

Dreyfuss JM, Oppenheimer SB (2011) Cyclodextrins and cellular interactions. In: Bilensoy E (ed) Cyclodextrins in pharmaceutics, cosmetics, and biomedicine: Current and future industrial applications. Wiley, Hoboken, pp 287–295

Durrant JD, McCammon JA (2011) Molecular dynamics simulations and drug discovery. BMC Biol 9:71. https://doi.org/10.1186/1741-7007-9-71

Elmes MW, Kaczocha M, Berger WT, Leung K-N, Ralph BP, Wang L, Sweeney JM, Miyauchi JT, Tsirka SE, Ojima I, Deutsch DG (2015) Fatty acid-binding proteins (FABPs) are intracellular carriers for Δ9-tetrahydrocannabinol (THC) and cannabidiol (CBD). J Biol Chem 290:8711–8721. https://doi.org/10.1074/jbc.M114.618447

Elms L, Shannon S, Hughes S, Lewis N (2019) Cannabidiol in the treatment of post-traumatic stress disorder: a case series. J Altern Complement Med 25:392–397. https://doi.org/10.1089/acm.2018.0437

Fasinu PS, Phillips S, El Sohly MA, Walker LA (2016) Current status and prospects for cannabidiol preparations as new therapeutic agents. Pharmacotherapy 36:781–796. https://doi.org/10.1002/phar.1780

Frank J, Holzwarth JF, Saenger W (2002) Temperature induced crystallization transition in aqueous solutions of β-cyclodextrin, heptakis(2,6-di-O-methyl)-β-cyclodextrin (DIMEB), and heptakis(2,3,6-tri-O-methyl)-β-cyclodextrin (TRIMEB) studied by differential scanning calorimetry. Langmuir 18:5974–5976. https://doi.org/10.1021/la020105a

Fraternali F, van Gunsteren WF (1996) An Efficient mean solvation force model for use in molecular dynamics simulations of

proteins in aqueous solution. J Mol Biol 256:939–948. https://doi.org/10.1006/jmbi.1996.0139
Freund TA, Katona IS, Piomelli D (2003) Role of endogenous cannabinoids in synaptic signaling. Physiol Rev 83:1017–1066. https://doi.org/10.1152/physrev.00004.2003
Friedman R (2011) Ions and the protein surface revisited: extensive molecular dynamics simulations and analysis of protein structures in alkali-chloride solutions. J Phys Chem B 115:9213–9223. https://doi.org/10.1021/jp112155m
Gidwani B, Vyas A (2015) A comprehensive review on cyclodextrin-based carriers for delivery of chemotherapeutic cytotoxic anticancer drugs. Biomed Res Int 2015:1–15. https://doi.org/10.1155/2015/198268
Goodwin ML, Harris JE, Hernández A, Gladden LB (2007) Blood lactate measurements and analysis during exercise: a guide for clinicians. J Diabetes Sci Technol 1:558–569. https://doi.org/10.1177/193229680700100414
Gunsteren WF, Mark AE (1992) On the interpretation of biochemical data by molecular dynamics computer simulation. Eur J Biochem 204:947–961. https://doi.org/10.1111/j.1432-1033.1992.tb16716.x
Hadland S, Knight JR, Harris SK (2015) Medical marijuana: review of the science and implications for developmental-behavioral pediatric practice. J Dev Behav Pediatr 36:115–123. https://doi.org/10.1097/dbp.0000000000000129
Halgren TA (1999) MMFF VI. MMFF94s option for energy minimization studies. MMFF VII. Characterization of MMFF94, MMFF94s, and other widely available force fields for conformational energies and for intermolecular-interaction energies and geometries. J Comput Chem 20:730–748. https://doi.org/10.1002/(SICI)1096-987X(199905)20:7<720:AID-JCC7>3.0.CO;2-X
Hammell DC, Zhang LP, Ma F, Abshire SM, McIlwrath SL, Stinchcomb AL, Westlund KN (2016) Transdermal cannabidiol reduces inflammation and pain-related behaviours in a rat model of arthritis. Eur J Pain 20:936–948. https://doi.org/10.1002/ejp.818
Hess B, Bekker H, Berendsen HJ, Fraaije JG (1997) LINCS: a linear constraint solver for molecular simulations. J Comput Chem 18:1463–1472. https://doi.org/10.1002/(SICI)1096-987X(199709)18:12<1463:AID-JCC4>3.0.CO;2-H
Hikiri S, Yoshidomme T, Ikeguch M (2016) Computational methods for configurational entropy using internal and cartesian coordinates. J Chem Theory Comput 12:5990–6000. https://doi.org/10.1021/acs.jctc.6b00563
Hingerty B, Klar B, Hardgrove GL, Betzel C, Saenger W (1984) Neutron diffraction of alpha, beta and gamma cyclodextrins: hydrogen bonding patterns. J Biomol Struct Dyn 2:249–260. https://doi.org/10.1080/07391102.1984.10507561
Horel JA (1996) Perception, learning and identification studied with reversible suppression of cortical visual areas in monkeys. Behav Brain Res 76:199–214. https://doi.org/10.1016/0166-4328(95)00196-4
Hubbard JI, Jones SF, Landau EM (1971) The effect of temperature change upon transmitter release, facilitation and post-tetanic potentiation. J Physiol 216:591–609. https://doi.org/10.1113/jphysiol.1971.sp009542
Humphrey W, Dalke A, Schulten K (1996) VMD: Visual molecular dynamics. J Molec Graphics 14:33–38. https://doi.org/10.1016/0263-7855(96)00018-5
Ichai C, Orban J-C, Fontaine E (2014) Sodium lactate for fluid resuscitation: the preferred solution for the coming decades? Crit Care 18:163. https://doi.org/10.1186/cc13973
Imamura K, Ogawa T, Sakiyama T, Nakanishi K (2003) Effects of types of sugar on the stabilization of protein in the dried state. J Pharm Sci 92:266–274. https://doi.org/10.1002/jps.10305
Iqbal U, Anwar H, Aftab M, Scribani M (2018) Ringer's lactate vs normal saline in acute pancreatitis: a systematic review and meta-analysis. J Dig Dis 113:S1–S2. https://doi.org/10.14309/00000434-201810001-00002
Ishiwata S, Kamiya M (1998) Temperature dependence and related properties of beta-cyclodextrin inclusion effects on the fluorescence intensities of hydroxycoumarin-based pesticides. Chemosphere 37:479–485. https://doi.org/10.1016/s0045-6535(98)00063-0
Jorgensen WL, Maxwell DS, Tirado-Rives J (1996) Development and testing of the OPLS all-atom force field on conformational energetics and properties of organic liquids. J Am Chem Soc 118:11225–11236. https://doi.org/10.1021/ja9621760
Kawabata Y, Wada K, Nakatani M, Yamada S, Onoue S (2011) Formulation design for poorly water-soluble drugs based on biopharmaceutics classification system: Basic approaches and practical applications. Int J Pharm 420:1–10. https://doi.org/10.1016/j.ijpharm.2011.08.032
Kitchen DB, Decornez H, Furr JR, Bajorath J (2004) Docking and scoring in virtual screening for drug discovery: methods and applications. Nat Rev Drug Discov 3:935–949. https://doi.org/10.1038/nrd1549
Kiyatkin EA (2019) Brain temperature and its role in physiology and pathophysiology: lessons from 20 years of thermorecording. Temperature (Austin) 6:271–333. https://doi.org/10.1080/23328940.2019.1691896
Koehler JE, Saenger W, van Gunsteren WF (1987) Molecular dynamics simulation of crystalline β-cyclodextrin dodecahydrate at 293 K and 120 K. Eur Biophys J 15:211–224. https://doi.org/10.1007/bf00577069
Kramer R, Shende V, Motl N, Pace C, Scholtz J (2012) Toward a molecular understanding of protein solubility: increased negative surface charge correlates with increased solubility. Biophys J 102:1907–1915. https://doi.org/10.1016/j.bpj.2012.01.060
Kreitzer AC, Regehr WG (2001) Cerebellar depolarization-induced suppression of inhibition is mediated by endogenous cannabinoids. J Neurosci 21:RC174–RC174. https://doi.org/10.1523/jneurosci.21-20-j0005.2001
Kumari R, Kumar R, Open Source Drug Discovery Consortium, Lynn A (2014) g_mmpbsa–a GROMACS tool for high-throughput MM-PBSA calculations. J Chem Inf Model 54:1951–1962. https://doi.org/10.1021/ci500020m
Lamparczyk H, Zarzycki PK (1995) Effect of temperature on separation of estradiol stereoisomers and equilin by liquid chromatography using mobile phases modified with β-cyclodextrin. J Pharm Biomed Anal 13:543–549. https://doi.org/10.1016/0731-7085(95)01324-E
Lee SC, Deutsch C (1990) Temperature dependence of K(+)-channel properties in human T lymphocytes. Biophys J 57:49–62. https://doi.org/10.1016/s0006-3495(90)82506-6
Lee JLC, Bertoglio LJ, Guimarães FS, Stevenson CW (2017) Cannabidiol regulation of emotion and emotional memory processing: relevance for treating anxiety-related and substance abuse disorders. Br J Pharmacol 174:3242–3256. https://doi.org/10.1111/bph.13724
Lenz RA, Wagner JJ, Alger BE (1998) N- and L-type calcium channel involvement in depolarization-induced suppression of inhibition in rat hippocampal CA1 cells. J Physiol 512:61–73. https://doi.org/10.1111/j.1469-7793.1998.061bf.x
Levenes C, Daniel H, Crepel F (2001) Retrograde modulation of transmitter release by postsynaptic subtype 1 metabotropic glutamate receptors in the rat cerebellum. J Physiol 537:125–140. https://doi.org/10.1111/j.1469-7793.2001.0125k.x
Li Y, Girard M, Shen M, Millan JA, Cruz MO (2017) Strong attractions and repulsions mediated by monovalent salts. Proc Natl Acad Sci 114:11838–11843. https://doi.org/10.1073/pnas.1713168114
Llano I, Leresche N, Marty A (1991) Calcium entry increases the sensitivity of cerebellar Purkinje cells to applied GABA and

decreases inhibitory synaptic currents. Neuron 6:565–574. https://doi.org/10.1016/0896-6273(91)90059-9

Maejima T, Hashimoto K, Yoshida T, Aiba A, Kano M (2001) Presynaptic inhibition caused by retrograde signal from metabotropic glutamate to cannabinoid receptors. Neuron 31:463–475. https://doi.org/10.1016/s0896-6273(01)00375-0

Maggio N, Stein ES, Segal M (2018) Cannabidiol regulates long term potentiation following status epilepticus: mediation by calcium stores and serotonin. Front Mol Neurosci 11:32. https://doi.org/10.3389/fnmol.2018.00032

Mannila J, Järvinen T, Järvinen K, Jarho P (2005) Effects of RM-β-CD on sublingual bioavailability of Δ9-tetrahydrocannabinol in rabbits. Eur J Pharm Sci 26:71–77. https://doi.org/10.1016/j.ejps.2005.04.020

Mannilla J, Järvinen T, Järvinen K, Jarho P (2007) Precipitation complexation method produces cannabidiol/beta-cyclodextrin inclusion complex suitable for sublingual administration of cannabidiol. J Pharm Sci 96:312–319. https://doi.org/10.1002/jps.20766

Matsuda H (1999) Cyclodextrins in transdermal and rectal delivery. Adv Drug Deliv Rev 36:81–99. https://doi.org/10.1016/s0169-409x(98)00056-8

Matsuda LA, Lolait SJ, Brownstein MJ, Young AC, Bonner TI (1990) Structure of a cannabinoid receptor and functional expression of the cloned cDNA. Nature 346:561–564. https://doi.org/10.1038/346561a0

Meng XY, Zhang HX, Mezei M, Cui M (2011) Molecular docking: a powerful approach for structure-based drug discovery. Curr Comput Aided Drug Des 7:146–157. https://doi.org/10.2174/157340911795677602

Miyamoto S, Kollman PA (1992) Settle: an analytical version of the SHAKE and RATTLE algorithm for rigid water models. J Comput Chem 13:952–962. https://doi.org/10.1002/jcc.540130805

Monnaert V, Tilloy S, Bricout H, Fenart L, Cecchelli R, Monflier E (2004) Behavior of alpha-, beta-, and gamma-cyclodextrins and their derivatives on an in vitro model of blood-brain barrier. J Pharmacol Exp Ther 310:745–751. https://doi.org/10.1124/jpet.104.067512

Morris GM, Huey R, Lindstrom W, Sanner MF, Belew RK, Goodsell DS, Olson AJ (2009) AutoDock4 and AutoDockTools4: automated docking with selective receptor flexibility. J Comput Chem 30:2785–2791. https://doi.org/10.1002/jcc.21256

Mundt N, Spehr M, Lishko PV (2018) TRPV4 is the temperature-sensitive ion channel of human sperm. Elife 7:e35853. https://doi.org/10.7554/eLife.35853

Munro S, Thomas KL, Abu-Shaar M (1993) Molecular characterization of a peripheral receptor for cannabinoids. Nature 365:61–65. https://doi.org/10.1038/365061a0

Murata N, Los DA (1997) Membrane fluidity and temperature perception. Plant Physiol 115:875–879. https://doi.org/10.1104/pp.115.3.875

Nimmo GR, Grant IS, Mackenzie SJ (1991) Lactate and acid base changes in the critically ill. Postgrad Med J 67:S56–S61

O'Boyle NM, Banck M, James CA, Morley C, Vandermeersch T, Hutchison GR (2011) Open Babel: an open chemical toolbox. J Cheminform 3:33. https://doi.org/10.1186/1758-2946-3-33

Ohlsson A, Lindgren J-E, Andersson S, Agurell S, Gillespie H, Hollister LE (1986) Single-dose kinetics of deuterium-labelled cannabidiol in man after smoking and intravenous administration. Biomed Environ Mass Spectrom 13:77–83. https://doi.org/10.1002/bms.1200130206

Pahari B, Chakraborty S, Sengupta PK (2018) Molecular insight into the inclusion of the dietary plant flavonol fisetin and its chromophore within a chemically modified γ-cyclodextrin: multi-spectroscopic, molecular docking and solubility studies. Food Chem 260:221–230. https://doi.org/10.1016/j.foodchem.2018.03.128

Payne VA, Xu J-H, Forsyth M, Ratner MA, Duward FS, Leeuw SW (1995a) Clustering in molecular dynamics simulations of sodium iodide solutions. Electrochim Acta 40:2087–2091. https://doi.org/10.1016/0013-4686(95)00145-5

Payne VA, Xu J-H, Forsyth M, Ratner MA, Duward FS, Leeuw SW (1995b) Molecular dynamics simulations of ion clustering and conductivity in NaI/ether solutions. I. Effect of ion charge. J Chem Phys 103:8734–8745. https://doi.org/10.1063/1.470130

Payne VA, Xu J-H, Forsyth M, Ratner MA, Duward FS, Leeuw SW (1995c) Molecular dynamics simulations of ion clustering and conductivity in NaI/ether solutions. II. Effect of ion concentration. J Chem Phys 103:8746–8755. https://doi.org/10.1063/1.470131

Peggion E, Mammi S, Palumbo M, Moroder L, Wünsch E (1983) Interaction of calcium ions with peptide hormones of the gastrin family. Biopolymers 22:2443–2457. https://doi.org/10.1002/bip.360221110

Pitler TA, Alger BE (1992) Postsynaptic spike firing reduces synaptic GABAA responses in hippocampal pyramidal cells. J Neurosci 12:4122–4132. https://doi.org/10.1523/jneurosci.12-10-04122.1992

Pitler TA, Alger BE (1994) Depolarization-induced suppression of GABAergic inhibition in rat hippocampal pyramidal cells: G protein involvement in a presynaptic mechanism. Neuron 13:1447–1455. https://doi.org/10.1016/0896-6273(94)90430-8

Riedel G, Davies SN (2005) Cannabinoid function in learning, memory and plasticity. In: Pertwee RG (ed) Cannabinoids. Handbook of experimental pharmacology. Springer, Berlin, Heidelberg, pp 445–477. https://doi.org/10.1007/3-540-26573-2_15

Rosa M, Roberts CJ, Rodrigues MA (2017) Connecting high-temperature and low-temperature protein stability and aggregation. PLoS ONE 12:e0176748. https://doi.org/10.1371/journal.pone.0176748

Saboury AA, Atri MS, Sanati MH, Moosavi-Movahedi AA, Hakimelahi GH, Sadeghi M (2006) A thermodynamic study on the interaction between magnesium ion and human growth hormone. Biopolymers 81:120–126. https://doi.org/10.1002/bip.20386

Schiff SJ, Somjen GG (1985) The effects of temperature on synaptic transmission in hippocampal tissue slices. Brain Res 345:279–284. https://doi.org/10.1016/0006-8993(85)91004-2

Serajuddin AT (2007) Salt formation to improve drug solubility. Adv Drug Deliv 59:603–616. https://doi.org/10.1016/j.addr.2007.05.010

Silvestro S, Mammana S, Cavalli E, Bramanti P, Mazzon E (2019) Use of cannabidiol in the treatment of epilepsy: efficacy and security in clinical trials. Molecules 24:1459. https://doi.org/10.3390/molecules24081459

Sipahiolgu O, Barringer SA, Taub I, Yang APP (2003) Characterization and modeling of dielectric properties of turkey meat. J Food Sci 68:521–527. https://doi.org/10.1111/j.1365-2621.2003.tb05705.x

Soares CM, Teixeira VH, Baptista AM (2003) Protein structure and dynamics in nonaqueous solvents: insights from molecular dynamics simulation studies. Biophys J 84:1628–1641. https://doi.org/10.1016/s0006-3495(03)74972-8

Steffens C, Kretschmann O, Ritter H (2007) Influence of cyclodextrin and temperature on the kinetics of free radical polymerization of N-adamantylacrylamide in water. Macromol Rapid Commun 28:623–628. https://doi.org/10.1002/marc.200600685

Stella VJ, He Q (2008) Cyclodextrins. Toxicol Pathol 36:30–42. https://doi.org/10.1177/0192623307310945

Sugiura T, Kondo S, Sukagawa A, Nakane S, Shinoda A, Itoh K, Waku K (1995) 2-Arachidonoylglycerol: a possible endogenous cannabinoid receptor ligand in brain. Biochem Biophys Res Commun 215:89–97. https://doi.org/10.1006/bbrc.1995.2437

Sugiura T, Yoshinaga N, Waku K (2001) Rapid generation of 2-arachidonoylglycerol, an endogenous cannabinoid receptor ligand, in rat brain after decapitation. Biochem Biophys Res Commun 297:175–178. https://doi.org/10.1016/s0304-3940(00)01691-8

Tong W, Wen H (2008) Applications of complexation in formulation of insoluble compounds. In: Liu R (ed) Water insoluble drug formulations, 2nd edn. Taylor and Francis Group, Boca Raton

Trott O, Olson AJ (2010) AutoDock Vina: improving the speed and accuracy of docking with a new scoring function, efficient optimization, and multithreading. J Comput Chem 31:455–461. https://doi.org/10.1002/jcc.21334

Uekama K, Hirayama F, Irie T (1998) Cyclodextrin drug carrier systems. Chem Rev 98:2045–2076. https://doi.org/10.1021/cr970025p

Uhernik AL, Montoya ZT, Balkissoon CD, Smith JP (2018) Learning and memory is modulated by cannabidiol when administered during trace fear-conditioning. Neurobiol Learn Mem 149:68–76. https://doi.org/10.1016/j.nlm.2018.02.009

Upadhye S, Kulkarni SJ, Majumdar S, Avery MA, Gul W, ElSohly MA, Repka MA (2010) Preparation and characterization of inclusion complexes of a hemisuccinate ester prodrug of Δ9-tetrahydrocannabinol with modified beta-cyclodextrins. AAPS Pharm Sci Tech 11:509–517. https://doi.org/10.1208/s12249-010-9401-4

Valle EM (2004) Cyclodextrins and their uses: a review. Process Biochem 39:1033–1046. https://doi.org/10.1016/s0032-9592(03)00258-9

Vazquez ML, Cepeda A, Prognon P, Mahuzier G, Blais J (1991) Cyclodextrins as modifiers of the luminescence characteristics of aflatoxins. Anal Chim Acta 255:343–350. https://doi.org/10.1016/0003-2670(91)80066-3

Vecsernyés M, Fenyvesi F, Bácskay I, Deli MA, Szente L, Fenyvesi É (2014) Cyclodextrins, blood-brain barrier, and treatment of neurological diseases. Arch Med Res 45:711–729. https://doi.org/10.1016/j.arcmed.2014.11.020

Vincent P, Armstrong CM, Marty A (1992) Inhibitory synaptic currents in rat cerebellar Purkinje cells: modulation by postsynaptic depolarization. J Physiol 456:453–471. https://doi.org/10.1113/jphysiol.1992.sp019346

Wardi Y (1988) A stochastic steepest-descent algorithm. J Optimi Theory App 59:307–323. https://doi.org/10.1007/bf00938315

Winkler RG, Fioravanti S, Ciccotti G, Margheritis C, Villa M (2000) Hydration of beta-cyclodextrin: a molecular dynamics simulation study. J Comput Aided Mol Des 14:659–667. https://doi.org/10.1023/a:1008155230143

Xu J-Y, Chen C (2015) Endocannabinoids in synaptic plasticity and neuroprotection. Neuroscientist 21:152–168. https://doi.org/10.1177/1073858414524632

Yang Y-M, Wang LY (2006) Amplitude and kinetics of action potential-evoked Ca^{2+} current and its efficacy in triggering transmitter release at the developing calyx of Held synapse. J Neurosci 26:5698–5708. https://doi.org/10.1523/jneurosci.4889-05.2006

Zasetsky AY, Svishchev IM (2001) Dielectric response of concentrated NaCl aqueous solutions: Molecular dynamics simulations. J Chem Phys 115:1448–1454. https://doi.org/10.1063/1.1381055

Ziance R, Chandler C, Bishara RH (2009) Integration of temperature-controlled requirements into pharmacy practice. J Am Pharm Assoc 49:e61–e69. https://doi.org/10.1331/japha.2009.081